

## Cardiac Anatomy and Physiology\*

PAUL S. PAGEL

DAVID F. STOWE

*\*From the Anesthesia Service, the Clement J. Zablocki Veterans Affairs Medical Center, Milwaukee, Wisconsin (PSP and DFS) and the Departments of Anesthesiology and Physiology, the Medical College of Wisconsin, Milwaukee, Wisconsin (DFS). This work was supported entirely by departmental funds. The authors have no conflicts of interest pursuant to this work. The authors thank our mentor and former Chairman John P. Kampine, MD, PhD, for his contributions to previous versions of this chapter.*

### KEY POINTS

- 1** The heart's cartilaginous skeleton, myocardial fiber orientation, valves, coronary blood supply, and conduction system determine its mechanical capabilities.
- 2** The cardiac myocyte is engineered for contraction and relaxation.
- 3** Changes in sarcomere muscle tension and length observed in isolated cardiac muscle are translated into alterations in pressure and volume in the intact heart.
- 4** The pressure-volume diagram provides a useful framework for the analysis of atrial and ventricular systolic and diastolic function.
- 5** The end-systolic and end-diastolic pressure-volume relations determine the operating range of each cardiac chamber.
- 6** Heart rate, preload, afterload, and myocardial contractility determine pump performance.
- 7** Preload is the quantity of blood that a chamber contains immediately before contraction.
- 8** Afterload is the external resistance to chamber emptying after contraction begins and the aortic valve opens.
- 9** Myocardial contractility is the force of contraction under controlled heart rate and loading conditions; contractility may be quantified using pressure-volume relation, isovolumic contraction, or ejection phase analysis.
- 10** The ability of a cardiac chamber to effectively collect blood at a normal filling pressure defines its diastolic function.
- 11** Diastole is a complex sequence of temporally related, heterogeneous events; no single index comprehensively describes diastolic function.
- 12** Left ventricular diastolic dysfunction is responsible for heart failure in as many as 50% of patients.
- 13** Invasive analysis of diastolic function may be conducted using the pressure-volume model.
- 14** Transmitral and pulmonary venous blood flow velocities derived using pulse wave Doppler echocardiography are commonly used to noninvasively measure diastolic function.
- 15** The restraining forces of the pericardium are important determinants of chamber filling and ventricular interdependence.
- 16** The atria are reservoirs, conduits, and contractile chambers.

## Introduction

The heart is a phasic, variable speed, electrically self-activating muscular pump that provides its own blood supply. The two pair of atria and ventricles are elastic chambers arranged in series that supply equal amounts of blood to the pulmonary and systemic vasculature. Myocardium in the atria and ventricles responds to stimulation rate and muscle stretch before (preload) and after (afterload) contraction begins. Coronary arterial blood vessels supply oxygen and metabolic substrates to the heart. The mechanical characteristics of the myocardium and its response to changes in autonomic nervous system activity allow the heart to adapt to rapidly changing physiologic conditions. The inherent contractile properties of the atria and ventricles and the ability of these chambers to adequately fill without excessive pressure are the major determinants of overall cardiac performance. As a result, abnormalities in either systolic or diastolic function may cause heart failure. Comprehensive knowledge of cardiac anatomy and physiology is essential for the practice of anesthesiology. This chapter describes the fundamentals of cardiac anatomy and physiology in adults. The authors will focus on the left atrium and ventricle (LA and LV, respectively) for the vast majority of the subsequent discussion unless otherwise noted.

## Gross Anatomy

### *Architecture*

**1** A flexible, cartilaginous structure forms the heart's skeleton composed of the annuli of the cardiac valves, the aortic and pulmonary arterial (PA) roots, the central fibrous body, and the left and right fibrous trigones. This foundation creates support for the valves and maintains the heart's structural integrity as internal pressures vary. A small quantity of superficial subepicardial muscle also inserts into the cartilaginous skeleton, but most atrial and ventricular muscle directly arises from and inserts within adjacent surrounding myocardium. Myocardial fibers are continuously interwoven and cannot be separated into distinct "layers." The atria contain two relatively thin orthogonal bands of myocardium, whereas the LV and, to a lesser extent the right ventricle (RV), consist of the interdigitating deep sinospiral, the superficial sinospiral, and the superficial bulbospiral muscles (Fig. 12-1). The angle of the myocardial fibers changes within the ventricular wall's thickness from the subendocardium to the subepicardium. Myocardial fibers of the LV are oriented in perpendicular, oblique, and helical planes from the cardiac base (superior in the mediastinum) to its apex. This arrangement reverses direction at approximately the LV's midpoint, creating an overall fiber architecture that mimics a flattened "figure of eight." This fiber orientation facilitates LV chamber shortening along the heart's longitudinal axis and produces a distinctive torsional twisting (analogous to "wringing" of a wash cloth) motion during contraction. The twisting effect substantially enhances the LV's ability to eject blood, as loss of this helical-rotational action reduces ejection fraction in patients with heart failure.<sup>1</sup> Elastic recoil of the systolic twist during LV relaxation is also an important determinant of early diastolic filling, especially during hypovolemia and exercise.<sup>2</sup> In contrast to the subepicardial and subendocardial layers, midmyocardial fibers are arranged in a circumferential orientation and act almost exclusively to decrease chamber diameter during contraction.

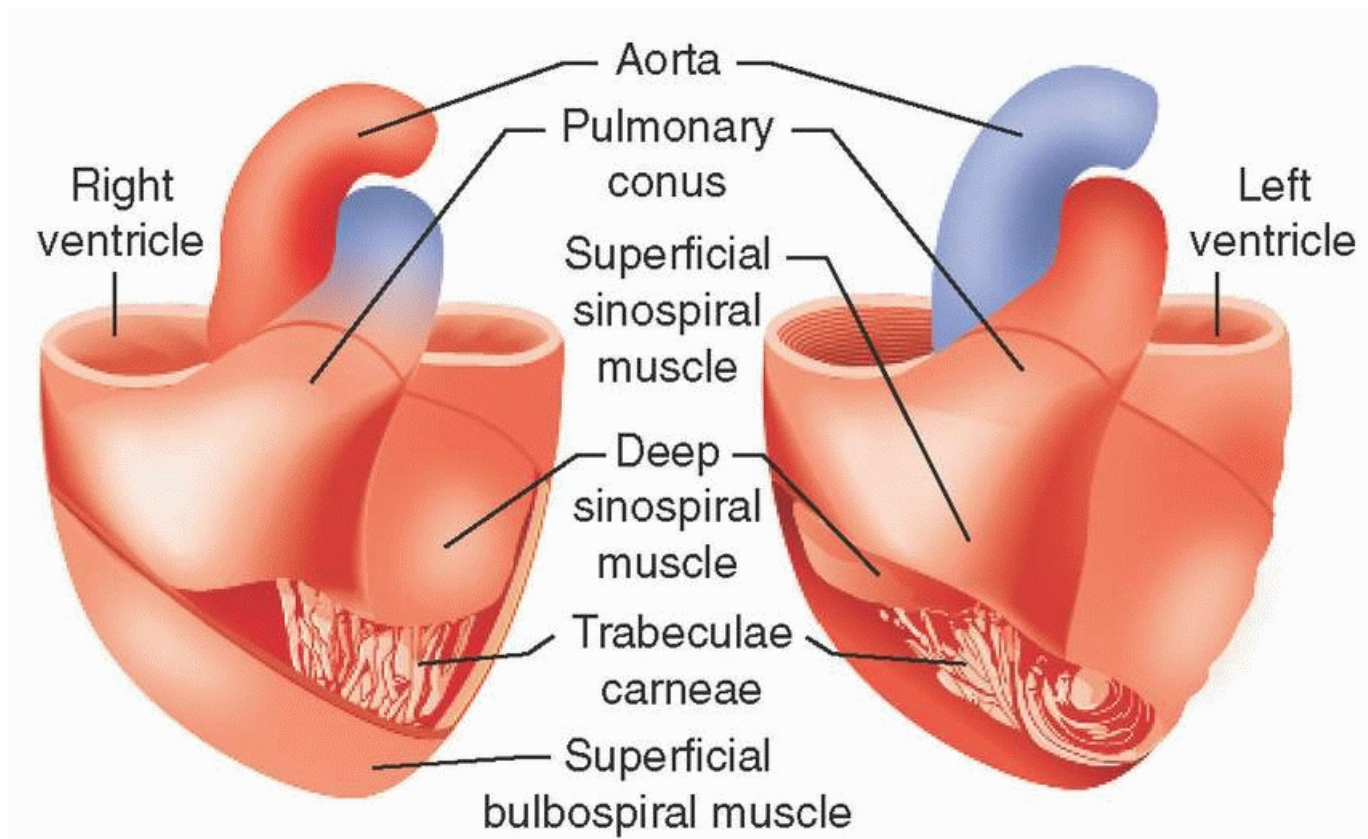


**Figure 12-1** Illustration depicting the components of the myocardium. The outer muscle layers pull the base of the heart toward the apex. The inner circumferential layers constrict the lumen, particularly of the LV.

The LV free walls taper in thickness from base to apex because the relative amount of midmyocardium gradually declines. LV and RV subendocardium and LV midmyocardium extending from the LV anterior wall contribute to the interventricular septum, which thickens toward the LV chamber during contraction under normal conditions because the majority of the septum is composed of LV myocardium. However, RV hypertrophy resulting from an increase in afterload (e.g., pulmonary arterial [PA] hypertension) may cause paradoxical motion of the interventricular septum. Regional differences in LV wall thickness and fiber orientation also contribute to load-dependent alterations in LV mechanics.<sup>3</sup> Irregular ridges of subendocardium (“trabeculae carneae” [Latin for “meaty ridges”]) are present within the RV chamber, and to a lesser extent, in the LV apex. The precise physiologic significance of the trabeculae carneae is unknown.

The LV apex and interventricular septum are relatively fixed in space within the mediastinum during contraction and relaxation. In contrast, the LV’s lateral and posterior walls shift position to the anterior and to the right during systole. This motion changes the orientation of the LV longitudinal axis from a position that favors LV filling (perpendicular to the mitral valve) to one that facilitates ejection (orthogonal to the LV outflow tract and aortic valve). The movement of the lateral and posterior LV walls during contraction is also responsible for the point of maximal impulse palpable on the left chest wall. The combined effects of subendocardial and subepicardial contraction, papillary muscle shortening, and elastic recoil produced by ejection of blood into the aortic root causes the LV base to descend toward the apex during contraction. Thus, normal electrical activation of the LV causes its long axis to shorten, reduces its chamber diameter, and produces torsional rotation of its apex in an anterior-right direction (Fig. 12-2). Differential changes in wall tension also create an apex-to-base intraventricular pressure gradient during LV ejection. This action enhances the transfer of stroke volume from the LV to the ascending aorta and proximal great vessels.

The crescent-shaped RV is located anterior and to the right of the LV. The RV propels venous blood into the compliant, low-pressure PA vasculature. The RV’s walls are thinner and contain fewer cardiac myocytes than the

LV. The RV is exposed to only 15% to 20% of the LV's peak systolic wall stress. Embryologically distinct inflow and outflow tracts exist in the RV. As a result, RV contraction is less temporally uniform than the LV and is more peristaltic in nature. The RV free wall uses the interventricular septum for structural support during contraction. The contracting LV also provides additional external assistance to RV during the latter chamber's contraction. These two factors combine to improve the RV's

P.279

mechanical advantage above its contractile ability alone, and in so doing, partially compensate for the chamber's thinner walls. This allows the RV to eject an identical stroke volume to the LV during each cardiac cycle. Nevertheless, the RV more easily decompensates when afterload increases because the RV is able to produce less than 20% of the total stroke work than the thicker, more muscular LV generates. However, the RV's greater compliance allows the chamber to more easily accommodate acute increases in preload than the stiffer LV.

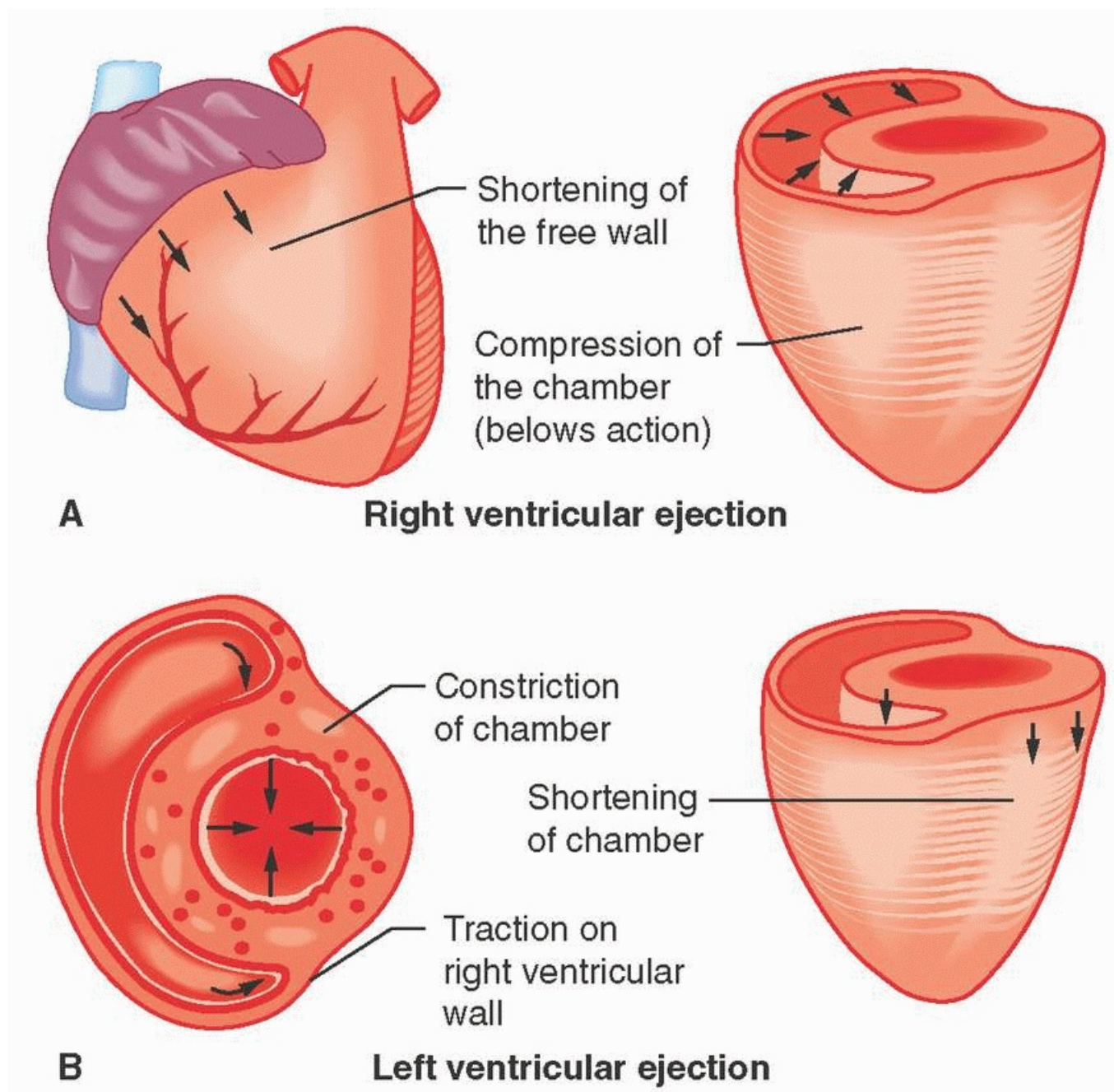


**Figure 12-2** Illustration depicting the contraction characteristics and modes of emptying of the RV and LV. The volumes ejected by each ventricle are equal, but the LV requires a more circumferential muscular wall to eject its volume at a pressure that is approximately four to five times greater than that in the right ventricle.

## **Valve Structure**

Two pairs of translucent, macroscopically avascular valves ensure unidirectional movement of blood through the normal heart. The pulmonic and aortic valves separate the RV and LV from the PA and aorta, respectively. The valves open and close passively in response to pressure gradients produced during contraction and relaxation, respectively. The pulmonic valve leaflets are named for their anatomic locations (right, left, and anterior), whereas the aortic valve leaflets correspond to the adjacent coronary artery ostium if present (right, left, and non). The orifice areas of the pulmonic and aortic valves are nearly equal to the corresponding cross-sectional areas of their annuli during ejection. The sinuses of Valsalva are dilated segments of aortic root immediately superior to each aortic leaflet. Hydraulic flow vortices occur within the sinuses that prevent adherence of the valve leaflets to the aortic wall during ejection and facilitate valve closure by preserving leaflet mobility during diastole.<sup>4</sup> These actions prevent the valve leaflets from inadvertently occluding the right and left coronary ostia. The proximal PA does not contain sinuses of Valsalva.

Located between the LA and the LV, the mitral valve has two leaflets (the oval-shaped anterior and the crescent-shaped posterior) and a prolapse ellipsoid (saddle-shaped) three-dimensional structure.<sup>5,6</sup> Coaptation of the leaflets occurs along a central curve with the anterior leaflet creating a convex border. Despite the differences in their shapes, the anterior and posterior leaflets have similar cross-sectional areas because the posterior leaflet occupies a greater percentage of the annular circumference. Anterior-lateral and posterior-medial commissures connect the leaflets in these annular locations and are located above each corresponding papillary muscle. A positive pressure gradient between the LA and LV develops during late LV relaxation as LV pressure falls below LA pressure, driving open the mitral valve and allowing blood to flow from the LA into the LV (early ventricular filling). LV untwisting and elastic recoil of the chamber further contribute to this process. The mitral valve closes as rapidly increasing LV hydraulic pressure during early systole forces the leaflets in a superior direction. The chordae tendinae act as restricting cables to limit this superior motion of the mitral leaflets, facilitating their coaptation. When functioning properly, the chordae tendinae prevent the mitral leaflets from prolapsing or inverting into the LA. Conversely, chordal rupture is a common cause of mitral regurgitation because excessive leaflet motion beyond the coaptation zone occurs, allowing unobstructed retrograde blood flow from the pressurized LV into the low-pressure LA outlet. Primary and secondary chordae tendinae attach to the leaflet edges and bodies, respectively, whereas tertiary chordae insert into the distal posterior leaflet or the myocardium immediately adjacent to the annulus. The papillary muscles are composed of subendocardial myocardium that contract with the LV. Each papillary muscle normally has chordal attachments to both mitral leaflets. Papillary muscle contraction tensions the chordae, providing another mechanism by which the chordae prevent excessive leaflet motion. Tightening of the mitral annulus through a sphincter-like contraction of the surrounding subepicardium also aids in mitral valve closure. The mitral valve apparatus is very important for normal LV function for two major reasons. First, the valve apparatus assures unidirectional blood flow from the LA to the LV by preventing reflux of blood into the LA and pulmonary veins during LV contraction. In addition to chordal rupture previously mentioned, papillary muscle ischemia or infarction may cause the mitral apparatus to fail, resulting in acute mitral regurgitation. Second, the mitral apparatus also contributes to LV systolic function because papillary muscle shortening assists LV apical contraction. This latter effect often becomes apparent during mitral valve replacement because many chordal attachments to the papillary muscles are intentionally severed. This compromise of mitral apparatus structure reduces LV ejection fraction and may contribute to difficult weaning from cardiopulmonary bypass in some patients undergoing mitral valve replacement, especially those with preexisting LV systolic dysfunction.

The tricuspid valve is normally composed of anterior, posterior, and septal leaflets.<sup>7</sup> The posterior leaflet is usually smaller than the anterior and septal leaflets. The tricuspid valve assures unidirectional movement of

blood from the RA and RV. Identification of a septal papillary muscle can be used to distinguish the morphologic RV from the LV in patients with some forms of congenital heart disease (e.g., transposition of the great vessels). A lateral segment of myocardium stretching between the apical aspects of anterior and septal papillary muscles, known as the moderator band, separates the embryologic RV inflow and outflow tracts. Unlike the mitral valve, the tricuspid valve does not have a collagenous annulus. Instead, the tricuspid leaflets originate from the atrioventricular groove that separates the RA from the RV. Notably, the proximal right coronary artery lies within this groove, and the vessel must be carefully avoided during tricuspid valve repair or replacement.

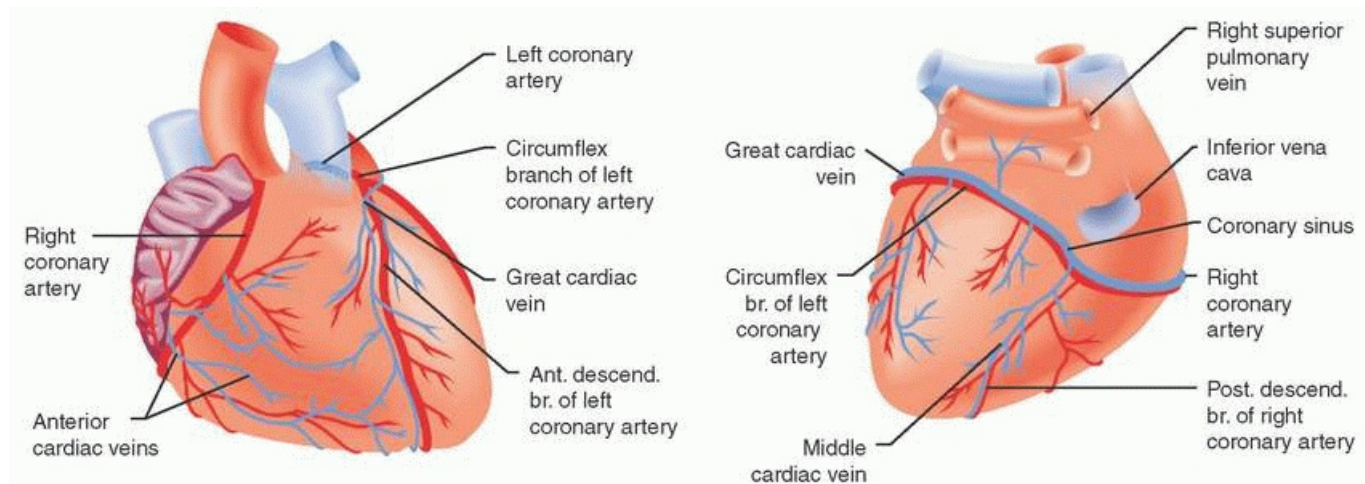


**Figure 12-3** An anterior view of the heart (left) shows right coronary and left anterior descending coronary arteries. A posterior view (right) shows left circumflex and posterior descending coronary arteries. The anterior cardiac veins from the RV and the coronary sinus, which drain primarily the LV, empty into the RA.

### **Coronary Blood Supply**

The left anterior descending, left circumflex, and right coronary arteries (LAD, LCCA, and RCA, respectively) supply blood to the LV (Fig. 12-3). Most coronary blood flow to the LV myocardium occurs during diastole because aortic pressure exceeds LV pressure. A critical stenosis or acute occlusion of the LAD, LCCA, or RCA almost invariably produces myocardial ischemia or infarction accompanied by regional contractile dysfunction that is easily predicted based on the known distribution of each coronary artery's blood supply. The LAD and its diagonal branches supply the medial LV anterior wall, the anterior two-thirds of the interventricular septum, and the LV apex. The LCCA and its marginal branches perfuse the anterior and posterior aspects of the lateral wall. The RCA provides blood flow to the medial portions of the posterior wall and the posterior one-third of the interventricular septum. The major epicardial coronary vessel that feeds the posterior descending coronary artery (PDA) determines the "dominance" of the coronary circulation. A "right dominant" circulation (RCA supplies blood to the PDA) is observed in approximately 80% of patients, whereas a "left dominant" circulation (LCCA perfuses the PDA) occurs in the remaining 20%. Distal connections or collateral vessels between the major coronary arteries may also provide an alternative route of blood flow to regions of myocardium that lie distal to a severe stenosis or occlusion. Notably, the development of coronary collaterals in response to chronic myocardial ischemia is highly variable and quite unpredictable in patients with coronary artery disease. A single coronary artery (2:1 ratio of RCA to LCCA) provides blood flow to the posterior-medial papillary muscle in two-thirds of patients. Thus, RCA or LCCA occlusion may produce acute posterior-medial papillary muscle ischemia or infarction and, as a result, new mitral regurgitation. However, this is not always the case, as both vessels perfuse the posteriormedial papillary muscle in the remaining patients.<sup>8</sup> In contrast to the variable blood supply to the posterior-medial papillary muscle, the anterior-lateral papillary muscle has a robust dual supply (LAD and LCCA), rendering this papillary muscle less susceptible to ischemic dysfunction than its counterpart.



Coronary blood flow to the RA, LA, and RV occurs during both systole and diastole because aortic pressure most often exceeds the pressure within each of these chambers unless profound hypotension is present (Fig. 12-4). The RCA and its branches supply blood flow to most of the RV, although distal diagonal and septal branches of the LAD also perfuse the RV anterior wall. Thus, either RCA or LAD occlusion may cause RV ischemia or infarction with resulting contractile dysfunction. Branches of the LCCA are the major sources of blood supply to the LA. As a result, LCCA occlusion often causes acute decompensation of LA contractility, whereas a compensatory increase in LA contractility

P.281

(based on a Frank-Starling mechanism) is most often observed if the LAD is acutely occluded.<sup>9</sup> Branches of both the RCA and the LCCA supply the RA. For example, either the RCA (55% of patients) or the LCCA perfuses the sinoatrial (SA) node. The RCA usually supplies blood to the atrioventricular (AV) node, but the LCCA may also perfuse the AV node depending on the coronary circulation's right or left dominance. The clinical implications of these relationships are clear: Critical stenosis or acute occlusion of either the RCA or LCCA may interrupt normal atrial or AV node conduction and cause bradyarrhythmias.

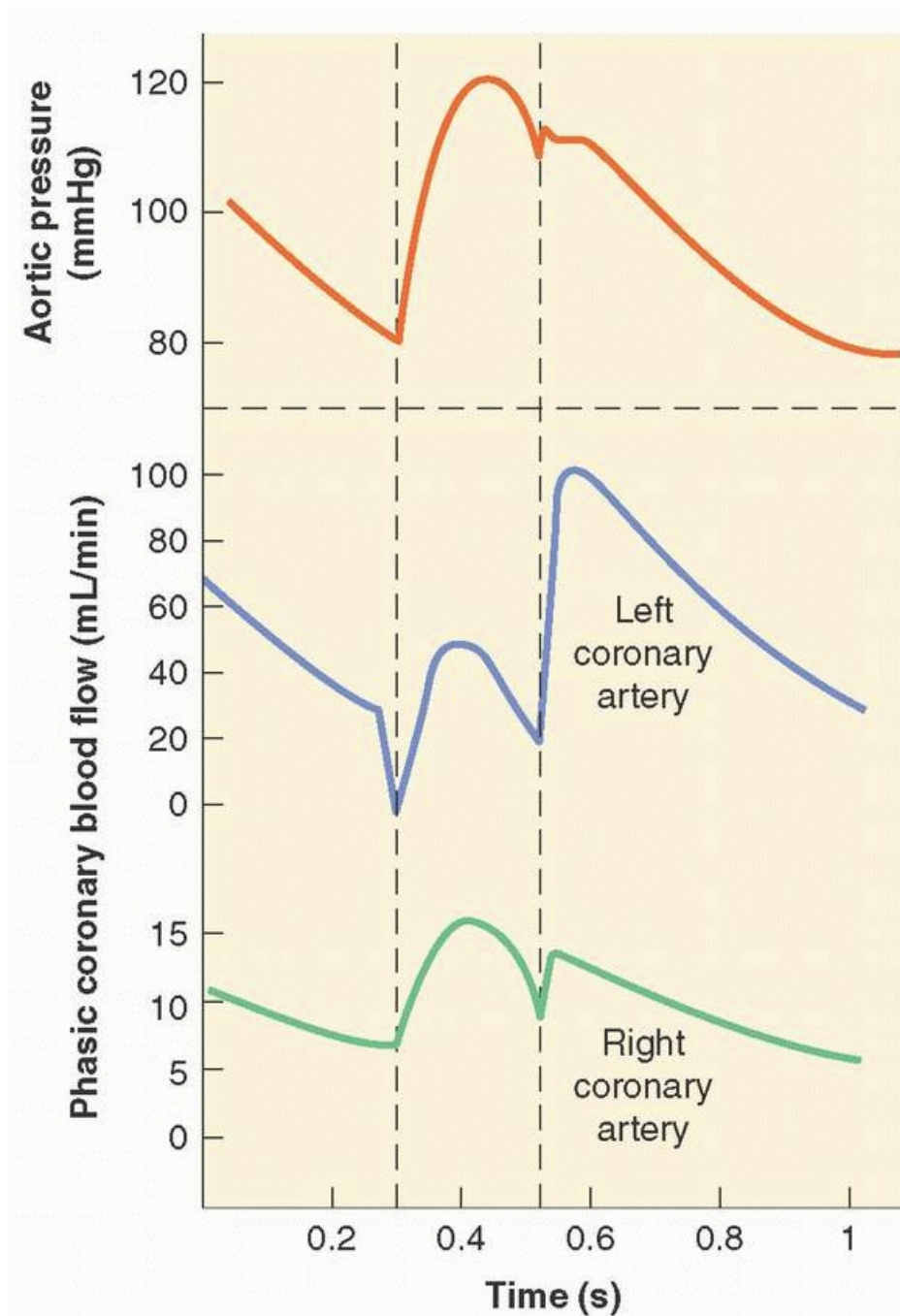


**Figure 12-4** Schematic representation of blood flow in the left and right coronary arteries during phases of the cardiac cycle. Note that most left coronary flow occurs during diastole while right coronary flow (and coronary sinus flow) occurs mostly during late systole and early diastole.

The proximal branches of the RCA, LCCA, and LAD are located on the epicardial surface of the heart and give rise to intramural vessels that penetrate perpendicularly or obliquely deep into the myocardium. Except for the thin tissue layer on the endocardial surface of each chamber, the heart's blood supply is derived almost entirely from perforating branches of the three major epicardial coronary arteries. The penetrating branches divide into dense capillary networks located parallel to the myocardial bundles. Arterial branches with diameters between 50 and 500  $\mu\text{m}$  form interconnecting anastomoses (Fig. 12-5), whereas vessels between 100 and 200  $\mu\text{m}$  in diameter form a plexus within the subendocardium. Coronary collaterals between different branches of the same coronary artery or between branches of two different coronary arteries are also variably present. Coronary collateral blood flow is usually minimal in the absence of a hemodynamically significant stenosis because the driving pressure across the collateral vessel is equal. However, if a main artery supplying one branch of a collateral vessel is severely stenotic or occluded, a pressure gradient develops that diverts blood flow from the patent artery into the myocardial distribution of the occluded artery through the collateral vessel. It stands to reason that the degree of coronary collateral formation often determines whether patients with coronary artery disease will develop anginal symptoms in response to increases in myocardial oxygen consumption.



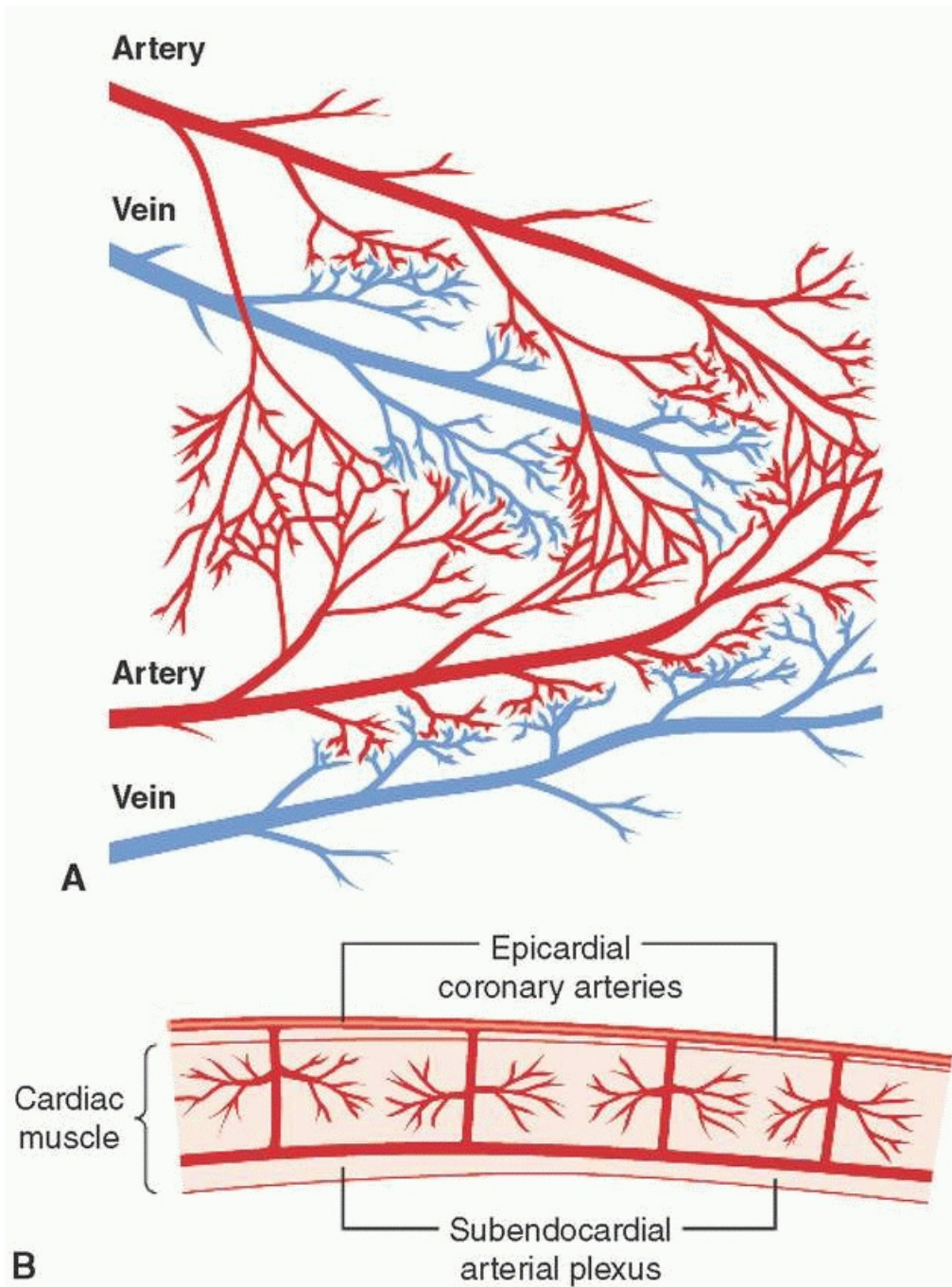


**Figure 12-5 A:** Diagram of the arterial-to-arterial and venous-to-venous anastomoses of the coronary arterial system, which allow diversion of flow if one distribution becomes blocked. **B:** Diagram of the epicardial coronary vessels lying on the cardiac muscle surface, the penetrating deep vessels, and the subendocardial arterial plexus connecting the deep vessels.

The main coronary venous drainage of the heart retraces the course of the major coronary arteries along the AV and interventricular grooves. There are three major coronary veins: the great cardiac vein courses along the AV groove and the LAD; the anterior cardiac vein is located adjacent to the RCA; and the middle cardiac vein is associated with PDA. Most often, there are two coronary veins located along either side of each major coronary arterial branch. The main coronary veins converge into the coronary sinus that empties into the posterior aspect of the right atrium immediately above the tricuspid valve.<sup>10</sup> Approximately 85% of total coronary blood flow returning from the LV empties into the coronary sinus, whereas the remaining flow drains directly into the atrial and ventricular cavities through the Thebesian veins. The RV veins drain into the anterior cardiac veins that empty individually into the RA.

The coronary capillary network is similar in structure to that observed in other tissue beds. The capillary to

myofibril density in myocardium is approximately 1:1 because of the heart's exceptionally high metabolic demand. Adjacent capillaries are usually separated by the diameter of single myocyte. The capillary distribution is quite uniform throughout the atria and ventricles (3,000 and 4,000/mm<sup>2</sup>) except in the AV node and interventricular septum, where it is substantially reduced. This observation provides an anatomic rationale explaining why the proximal portion of the RV and LV conduction system may be more vulnerable to ischemia. As in other capillary beds, coronary capillaries are the sites for oxygen and carbon dioxide exchange and for the movement of larger molecules (e.g., glucose) across the endothelium without the impediment of vascular smooth muscle.

## ***Impulse Conduction***



The mechanism by which the heart is electrically activated is critical for its performance. The SA node is the primary cardiac pacemaker. Decreases in firing rate, delays or blockade of normal conduction, or the presence of secondary pacemakers (e.g., AV node, bundle of His) may supersede the dominance of SA automaticity. The anterior, middle (Wenckebach), and posterior (Thorel) internodal pathways rapidly transmit the initial SA node depolarization across the RA to the AV node. Bachmann's bundle (a branch of the anterior internodal pathway) transmits the SA node depolarization across the LA through the atrial septum. Histologic examination of atrial myocytes rarely allows differentiation of cells that are specifically involved in the internodal pathway, but the unique conducting characteristics of these specialized myocytes may be clearly identified in the electrophysiology laboratory. The heart's cartilaginous skeleton electrically isolates the atria from the ventricles. As a result, atrial depolarization is directed solely to the RV and LV through the AV node, which pierces this cartilaginous framework. Because AV node conduction velocity is quite slow compared with the pathways proximal and distal to it, the AV node is responsible for the sequential contraction pattern of the atria and the ventricles. Accessory pathways that bypass the AV node and establish abnormal conduction between the atria and ventricles may precipitate supraventricular tachyarrhythmias. This is the putative mechanism

P.282

by which the bundle of Kent produces Wolff-Parkinson-White syndrome. The AV node transmits its depolarization to the His bundle, which further transmits the signal to the RV and LV via the right and left bundle branches, respectively, through Purkinje fibers within the endocardium. The conduction velocity through the His bundle, the bundle branches, and the Purkinje network is very rapid, assuring coordinated RV and LV depolarization and contraction. The relatively homogeneous distribution of Purkinje fibers throughout the LV myocardium produces temporally uniform contractile activation of the chamber (functional syncytium). Notably, artificial RV epicardial pacing (as is sometimes used during cardiac surgery) does not rely on this normal conduction sequence and, as a result, causes dyssynchronous LV activation that may be erroneously interpreted as a new ischemia-induced regional wall motion abnormality. Chronic RV apical pacing may also contribute to LV dysfunction and subsequent heart failure because of long-term imposition of contractile dyssynchrony.<sup>11</sup> Indeed, restoration of the normal electrical activation sequence is the basis upon which cardiac resynchronization therapy improves LV contractile function in patients with heart failure.<sup>12</sup>

[View Quicktime Video](#)

12.1 Junctional Rhythm

[View Quicktime Video](#)

12.2 Wolff-Parkinson White Syndrome

## **Coronary Physiology**

Blood supply to the LV is directly dependent on the difference between the aortic diastolic pressure and LV end-diastolic pressure (coronary perfusion pressure) and inversely related to the vascular resistance to flow, which varies to the fourth power of the vessel radius (Poiseuille law). Two other determinants of coronary flow are vessel length and blood viscosity, but these factors are relatively constant. Resting coronary blood flow in the adult is approximately 250 mL/min (1 mL/min/g; 5% of normal adult cardiac output). Cyclical changes in aortic pressure and the resistance to flow resulting from physical compression of the intramural coronary arteries govern the pulsatile pattern of LV coronary flow. The LV subendocardium is exposed to a higher pressure than the subepicardium during systole, and the intraventricular tissue pressure actually exceeds peak developed LV pressure. As a result, the subendocardial layer is much more susceptible to ischemia when a flow-limiting coronary stenosis, pressure-overload hypertrophy, or pronounced tachycardia is present. Coronary blood flow is also reduced when aortic diastolic pressure is low, such as occurs in severe aortic valvular insufficiency. Elevated LV end-diastolic pressure, as typically observed in heart failure, also reduces coronary perfusion pressure and blood flow. Venous blood flow in the coronary sinus peaks during late systole because the contracting LV compresses major venous drainage channels.

Another important determinant of coronary blood flow is coronary vascular resistance (estimated using the ratio of coronary blood flow to perfusion pressure), which also varies substantially during the cardiac cycle. While coronary perfusion certainly changes in response to aortic, intramyocardial, and coronary venous pressures, the primary regulator of coronary blood flow is the variable resistance imparted by coronary vascular smooth muscle. For example, activation of the sympathetic nervous system increases coronary vascular smooth muscle tone, thereby making coronary vascular resistance greater. The degree of smooth muscle stretch (myogenic factor) also influences coronary vascular tone and resistance. However, metabolic factors are the primary physiologic determinants of coronary vascular tone and myocardial perfusion. The ratio of subepicardial to subendocardial blood flow remains near unity throughout the cardiac cycle despite the differentially greater systolic compressive forces exerted on the subendocardium.  $\beta$  adrenoceptor-mediated vasodilation and local release of metabolic autocrine substances (e.g., adenosine) produced by the myocardium itself act to offset this greater resistance to flow in the subendocardium. The relative maintenance of subendocardial blood flow despite compression is also related to the redundancy of arteriolar and capillary anastomoses within the subendocardium.

The heart normally extracts between 75% and 80% of arterial oxygen content, by far the greatest oxygen extraction of all the body's organs. The majority of myocardial oxygen consumption results from the magnitude of LV pressure during isovolumic contraction and the rate at which this pressure develops. The LV's diameter and wall thickness also have profound effects on myocardial oxygen consumption as dictated by the Law of Laplace (see below). Heart rate is the primary determinant of myocardial oxygen consumption in the intact heart. Increases in myocardial contractility, preload, and afterload are also associated with greater myocardial oxygen consumption. Cardiac oxygen extraction is near maximal under resting conditions and cannot substantially increase during exercise. As a result, the primary mechanism by which myocardium is able to meet its oxygen requirements during exercise is through enhanced oxygen delivery, which is proportional to coronary blood flow when hemoglobin concentration is constant. Thus, it is not surprising that myocardial oxygen consumption is the most important determinant of coronary blood flow. For example, myocardial oxygen consumption and corresponding coronary blood flow increase by a magnitude of four- to fivefold during strenuous physical exercise. The difference between maximal and resting coronary blood flow (coronary reserve) determines the magnitude with which coronary blood flow can rise during exercise-induced increases in myocardial oxygen consumption. Coronary vascular resistance is greater in the resting, perfused heart than in the contracting heart. These data suggest that increases in coronary blood flow exceed those of perfusion pressure in response to greater myocardial oxygen consumption when the heart is contracting versus when it is quiescent. The precise mechanisms responsible for this close correlation between myocardial oxygen consumption and coronary vasomotor tone remain elusive. The factors responsible for coronary autoregulation (maintenance of coronary

blood flow despite changes in perfusion pressure) and reactive hyperemia (the several-fold increase in coronary blood flow above baseline after a brief period of myocardial ischemia) are also not clearly understood. Metabolic coronary vasodilation in response to enhanced myocardial oxygen consumption during exercise occurs, at least in part, as a result of enhanced local release of metabolic substrates (e.g., adenosine, ADP) combined with sympathetic nervous system stimulation of the coronary vasculature. This latter effect causes a “feed-forward” vasodilation of small coronary arterioles by activating  $\beta$  adrenoceptors.<sup>13</sup> An  $\alpha$  adrenoceptor-induced vasoconstriction also occurs in larger coronary arteries during exercise. Although seemingly counterintuitive, this differential vasoconstriction of larger caliber upstream coronary arteries serves two important functions: reduction of vascular compliance and attenuation of the wide swings in coronary blood flow normally observed during the cardiac cycle. These actions act to preserve coronary perfusion to the more vulnerable LV subendocardium when heart rate, inotropic state, and myocardial oxygen consumption are elevated. In contrast to the important role of the cardiac sympathetic nerves, parasympathetic innervation has a relatively minor direct effect on coronary blood flow regulation despite its well-known negative inotropic and chronotropic actions.

The aforementioned conclusions about sympathetic nervous system control of the coronary circulation are based on alterations in the slope of the myocardial oxygen consumption-coronary venous oxygen tension relation during graded exercise in the presence of exogenous  $\alpha$  or  $\beta$  adrenoceptor blockade. The  $\beta$  adrenoceptor appears to account for only one-fourth of the

P.283

total coronary vasodilation observed during exercise-induced hyperemia, but most of this vasodilation is most likely related to local or autocrine metabolic factors that act on coronary vascular smooth muscle with or without the additional modulation by vascular endothelium. Adenine nucleotides from red blood cells or the myocardium itself may activate endothelial purinergic receptors to produce coronary vasodilation during exercise.<sup>14</sup> Many factors have been proposed to individually or collectively modulate coronary blood flow at the arteriolar or capillary level, including adenosine, bradykinin, nitric oxide, arterial oxygen or carbon dioxide tension, acid-base status, osmolarity, plasma electrolyte (e.g.,  $K^+$ ,  $Ca^{2+}$ ) concentrations, and various products of arachidonic acid metabolism. Many of these factors exert predictable direct effects. For example, hypoxia or ischemia decreases arterial oxygen tension and pH concomitant with increases in carbon dioxide tension, adenosine release, and the plasma concentrations of  $K^+$  and  $Ca^{2+}$ . These changes collectively augment coronary blood flow during exercise, but none individually is solely responsible for this vasodilation. Adenosine receptor blockade does not alter coronary blood flow under resting conditions or during exercise. Similarly, inhibition of nitric oxide (NO) production or antagonism of adenosine triphosphate-sensitive potassium ( $K_{ATP}$ ) channels does not affect the myocardial oxygen consumption-coronary venous oxygen content relationship during graded exercise. Nevertheless, it is quite clear that NO and  $K_{ATP}$  channels are important regulators of myocardial oxygen supply-demand relations under resting conditions. Adenosine released during hypoxia or ischemia also causes coronary vasodilation, and  $K_{ATP}$  channel activation mediates this effect. Adenosine and  $K_{ATP}$  channels also play a central role in reactive hyperemia after brief myocardial ischemia, but neither mediator appears to be required for coronary autoregulation. Indeed, the  $K_{ATP}$  channel may act to reduce coronary vascular smooth muscle tone and maintain a higher basal level of coronary blood flow during resting conditions. While not acting as a local metabolic vasodilator of small coronary arteries and arterioles per se, NO may dilate larger epicardial coronary vessels in response to downstream vasodilation and prevent excessive sheer stress on coronary vascular endothelium. Endothelin and thromboxane  $A_2$  produce direct coronary vasoconstriction in vitro, but the precise role of these substances on the regulation of coronary blood flow in vivo has not been defined.

## Cardiac Myocyte Anatomy and Function

## **Ultrastructure**

**2** The heart contracts and relaxes nearly three billion times during an average lifetime, based on an average heart rate of 70 beats per minute and a life expectancy of 75 years. A review of cardiac myocyte ultrastructure provides important insights into how this remarkable feat is possible. The sarcolemma is the external membrane of the cardiac muscle cell. The sarcolemma contains ion channels (e.g.,  $\text{Na}^+$ ,  $\text{K}^+$ ,  $\text{Ca}^{2+}$ ), ion pumps and exchangers (e.g.,  $\text{Na}^+$ - $\text{K}^+$  ATPase,  $\text{Ca}^{2+}$ -ATPase,  $\text{Na}^+$ - $\text{Ca}^{2+}$  or  $\text{Na}^+$ - $\text{H}^+$  exchangers), G protein-coupled and other receptors (e.g.,  $\beta_1$  adrenergic, muscarinic, adenosine, opioid), and transporter enzymes that regulate intracellular ion concentrations, facilitate signal transduction, and provide metabolic substrates required for energy production. Deep invaginations of the sarcolemma, known as transverse (T) tubules, penetrate the internal structure of the myocyte at regular intervals. The T-tubules assure rapid, simultaneous transmission of the depolarizing impulses that initiate myocyte contraction. The cardiac myocyte is densely packed with mitochondria that are responsible for production of large quantities of high-energy phosphates (e.g., ATP) needed for contraction and relaxation. The sarcomere is the fundamental contractile unit of cardiac muscle. The myofilaments within each sarcomere are arranged in parallel cross-striated bundles of thin (containing actin, tropomyosin, and the troponin complex) and thick (primarily composed of myosin and its supporting proteins) fibers. Sarcomeres are connected in series and produce characteristic shortening and thickening of the long and short axes of each myocyte, respectively, during contraction.

Observations from light and electron microscopy led to the definition of the sarcomere's distinctive structural features. The area of overlap of thick and thin fibers characterizes the "A" band. This band lengthens as the sarcomere shortens during contraction. The "I" band represents the region of the sarcomere that contains thin filaments alone, and this band is reduced in width as the cell contracts. Each "I" band is bisected by a "Z" (from the German *zuckung* [twitch]) line, which delineates the border between two adjacent sarcomeres. As a result, the length of each sarcomere contains a complete "A" band and two symmetric one-half "I" bands located between "Z" lines. A central "M" band is also present within the "A" band. This "M" band is composed of thick filaments spatially constrained in a cross-sectional hexagonal matrix by myosin-binding protein C. A densely intertwined network of sarcoplasmic reticulum (SR) invests each bundle of contractile proteins and functions as a  $\text{Ca}^{2+}$  reservoir. This SR network assures homogeneous distribution and reuptake of activator  $\text{Ca}^{2+}$  throughout the myofilaments during contraction and relaxation, respectively. The SR subsarcolemmal cisternae are specialized structures located immediately adjacent to, but not continuous with, the sarcolemmal and transverse tubular membranes. The cisternae are packed with ryanodine receptors that function as the primary  $\text{Ca}^{2+}$  release channel for the SR. The contractile machinery and the mitochondria that power it occupy more than 80% of the total volume of the cardiac myocyte. This observation emphasizes that mechanical function, and not new protein synthesis, is the predominant activity of the cardiac myocyte. Intercalated discs connect adjacent myocytes through the fascia adherens and desmosomes that link actin and other proteins between cells, respectively. The intercalated discs also provide a seamless electrical connection between myocytes via large, nonspecific ion channels (known as "gap junctions") that facilitate intercellular cytosolic diffusion of ions and small molecules.

## **Contractile Apparatus**

Myosin, actin, tropomyosin, and the three-protein troponin complex compose the six major components of the contractile apparatus. Myosin (molecular weight of approximately 500 kDa; length, 0.17  $\mu\text{m}$ ) contains two interwoven chain helices with two globular heads that bind to actin and two additional pairs of light chains. Enzymatic digestion of myosin divides the structure into light (containing the tail section of the complex) and heavy (composed of the globular heads and the light chains) meromyosin. The elongated tail section of the

myosin complex (light meromyosin) functions as the main structural support of the molecule (Fig. 12-6). The globular heads of the myosin dimer contain two “hinges,” located at the junction of the distal light chains and the tail helix, that play an essential role in myofilament shortening during contraction. These globular structures bind to actin, thereby activating an ATPase that is involved in hinge rotation and release of actin during contraction and relaxation, respectively. The activity of this actin-activated myosin ATPase is a

P.284

major determinant of the maximum velocity of sarcomere shortening. Notably, adult and neonatal atrial and ventricular myocardium contain several different myosin ATPase isoforms that are distinguished by their relative ATPase activity. The myosin molecules are primarily arranged in series along the length of the thick filament, but are abutted “tail-to-tail” in the center of the thick filament. This orientation facilitates shortening of the distance between “Z” lines during contraction as the thin filaments are drawn symmetrically toward the sarcomere's center.

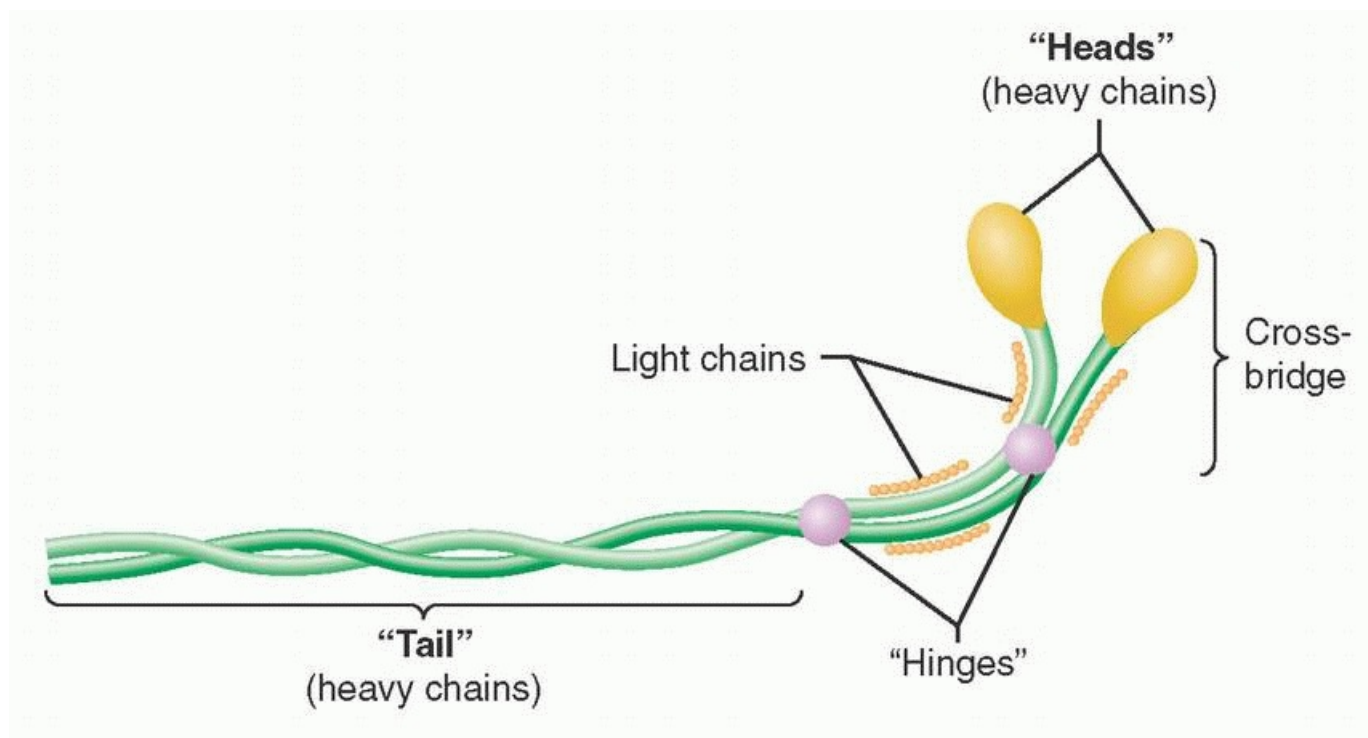


**Figure 12-6** Schematic illustration of the myosin molecule demonstrating double helix tail, globular heads that form cross bridges with actin during contraction, two pairs of light chains, and “hinges” (cleavage sites of proteolytic enzymes) that divide the molecule into meromyosin fragments (see text).

The light chains contained within the myosin complex serve “regulatory” or “essential” roles. Regulatory myosin light chains may favorably modulate myosin-actin interaction through  $\text{Ca}^{2+}$ -dependent protein kinase phosphorylation, whereas essential light chains serve an as yet undefined obligate function in myosin activity because their removal denatures the myosin molecule. Discussion of myosin light chain isoforms is beyond the scope of this chapter, but it is important to note that isoform switches from ventricular to atrial forms have been observed in left ventricular hypertrophy that may contribute to contractile dysfunction.<sup>15</sup> In addition to myosin and its binding protein, thick filaments contain titin, a long elastic protein that attaches myosin to the “Z” lines. Titin is thought to be a “length sensor” that establishes progressively greater passive restoring forces as sarcomere length approaches its maximum or minimum (similar to a bidirectional spring).<sup>16</sup> Compression and stretching of titin occur during decreases and increases in muscle load, thereby resisting further sarcomere shortening and lengthening, respectively. Thus, titin is a third important elastic element (in addition to actin and myosin) that contributes to the stress-strain mechanical properties of cardiac muscle.<sup>17</sup>

Actin is the major component of the thin filament. Actin is a 42-kDa, ovoid-shaped, globular protein ("G" form; 5.5 nm in diameter) that exists as a filamentous (F) polymer in cardiac muscle. F-actin binds ADP and a divalent cation ( $\text{Ca}^{2+}$  or  $\text{Mg}^{2+}$ ), but unlike myosin, the molecule does not directly hydrolyze high-energy nucleotides (e.g., ATP). F-actin is wound in double-stranded helical chains of G-actin monomers that resemble two intertwined strands of pearls. A single complete helical revolution of filamentous actin is approximately 77 nm in length and contains 14 G-actin monomers. Actin derives its name from its function as the "activator of myosin" ATPase through its reversible binding with myosin. The hydrolysis of ATP by this actin-myosin complex provides the chemical energy required to produce the conformational changes in the myosin heads that drive the contraction-relaxation cycle within the sarcomere. Tropomyosin is one of two major inhibitors of actin-myosin interaction. Tropomyosin (length of 40 nm; weight between 68 and 72 kDa) is a rigid double-stranded  $\alpha$ -helix protein. A single disulfide bond links the two helices of tropomyosin. Human tropomyosin contains both  $\alpha$  and  $\beta$  isoforms (34 and 36 kDa, respectively) and may be present as a homo- or heterodimer.<sup>18</sup> Tropomyosin serves to stiffen the thin filament through its position within the longitudinal cleft between intertwined F-actin polymers (Fig. 12-7). However, the primary function of tropomyosin is its  $\text{Ca}^{2+}$ -dependent interaction with troponin complex proteins. This tropomyosin-troponin interaction provides the microscopic link between sarcolemmal membrane depolarization to actin-myosin binding (excitation-contraction coupling). Cytoskeletal proteins, including actinin and nebulin, anchor the thin filaments to the "Z" lines.<sup>19</sup>

The troponin proteins serve complementary yet distinct roles as regulators of the contractile apparatus.<sup>20</sup> The troponin complexes are arranged at 40-nm intervals along the length of the thin filament. Troponin C (so named because this molecule binds  $\text{Ca}^{2+}$ ) exists in a highly conserved, single isoform in cardiac muscle. Troponin C is composed of a central nine-turn  $\alpha$  helix separating two globular regions that contain four discrete amino acid sequences capable of binding divalent cations. Two (termed sites I and II) of the four amino acid-cation binding sequences are  $\text{Ca}^{2+}$ -specific. This feature allows the troponin C molecule to respond to the acute changes in intracellular  $\text{Ca}^{2+}$  concentration that accompany contraction and relaxation. Cardiac troponin I (inhibitor) is a 23-kDa protein that exists in a single isoform. Troponin I alone weakly prevents the interaction between actin and myosin, but when combined with tropomyosin, the troponin I-tropomyosin complex becomes the primary inhibitor of actin-myosin binding. Troponin I contains a serine residue that may be phosphorylated by protein kinase A via cAMP, reducing troponin C- $\text{Ca}^{2+}$  binding and enhancing relaxation during administration

P.285

of  $\beta_1$  adrenoceptor agonists (e.g., dobutamine) or phosphodiesterase fraction III inhibitors (e.g., milrinone).

Troponin T (so named because it binds other troponin molecules and tropomyosin) is the largest of the troponin proteins and exists in four major isoforms. Troponin T anchors the other troponin molecules and influences the relative  $\text{Ca}^{2+}$  sensitivity of the complex.<sup>21</sup>

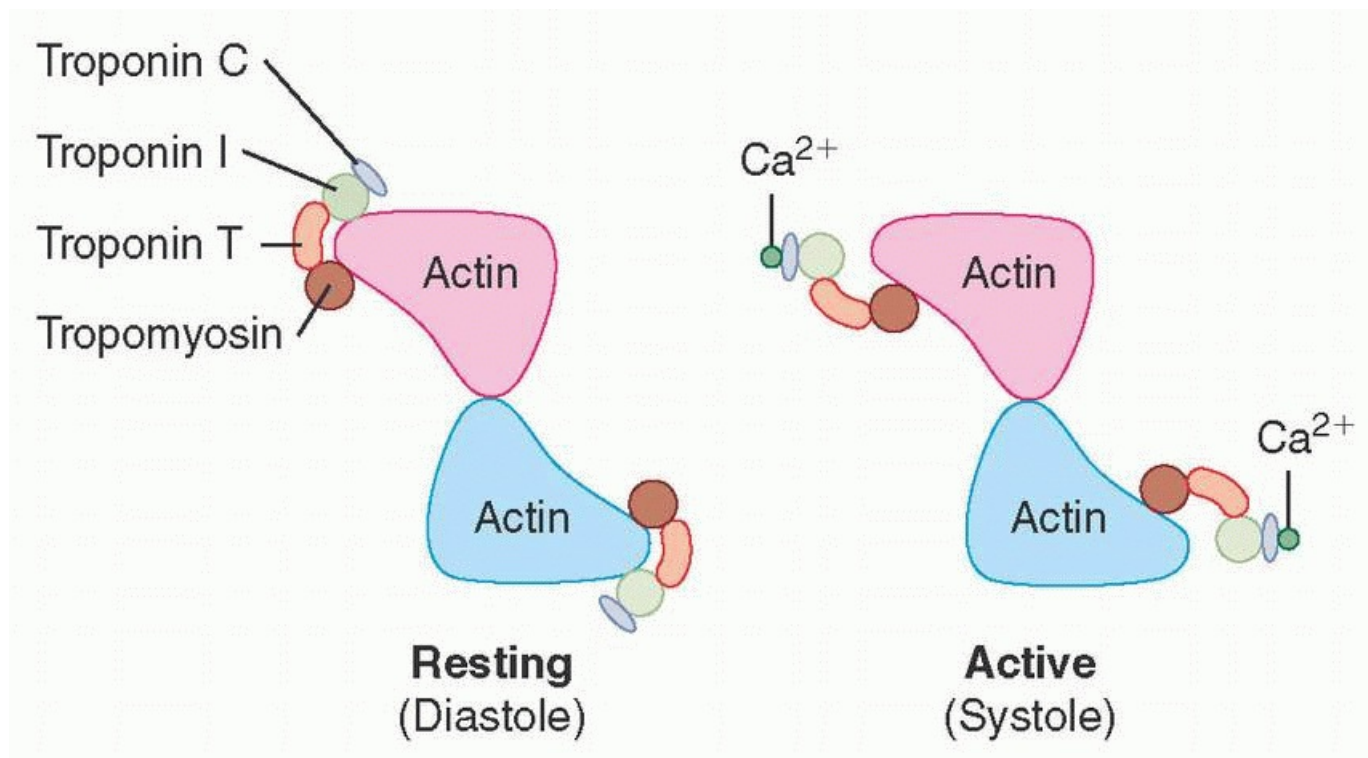


**Figure 12-7** Cross-sectional schematic illustration demonstrating the structural relationship between the troponin-tropomyosin complex and actin under resting conditions (left panel) and after Ca<sup>2+</sup> binding to troponin C (right panel, see text).

### ***Calcium-Myofilament Interaction***

A series of conformational changes in the troponin-tropomyosin complex occur as a result of Ca<sup>2+</sup>-troponin C binding that culminate in exposure of the myosin-binding site on the actin molecule. During conditions in which intracellular Ca<sup>2+</sup> concentration is low (10<sup>-7</sup> M; diastole), very little Ca<sup>2+</sup> is bound to troponin C, and a troponin complex constrains each tropomyosin molecule to the outer region of the groove between F-actin filaments. This configuration blocks cross-bridge formation and prevents myosin-actin interaction. Thus, the troponin-tropomyosin complex creates a basal inhibitory state under resting conditions. A 100-fold increase in intracellular Ca<sup>2+</sup> concentration (10<sup>-5</sup> M) occurs as a result of sarcolemmal depolarization (systole). Opening of L- and T-type sarcolemmal Ca<sup>2+</sup> channels allows Ca<sup>2+</sup> influx into the myocyte from the extracellular compartment and stimulates Ca<sup>2+</sup>-dependent Ca<sup>2+</sup> release from the SR through its ryanodine receptors. When Ca<sup>2+</sup> is bound to troponin C, troponin C elongates and its interactions with troponin I and T are enhanced. This allosteric rearrangement and the altered binding characteristics that it produces weaken the interaction between troponin I and actin, allow repositioning of the tropomyosin molecule along the F-actin filaments, and reverse the baseline inhibition of actin-myosin binding by tropomyosin.<sup>22</sup> As a result, Ca<sup>2+</sup> binding to troponin C is directly linked to a series of changes in regulatory protein structure, negating inhibition of the binding site for myosin on the actin molecule and allowing cross-bridge formation to occur. This antagonism of inhibition is fully reversible: Ca<sup>2+</sup> dissociation from troponin C restores the original troponin-tropomyosin conformation on F-actin and facilitates relaxation.



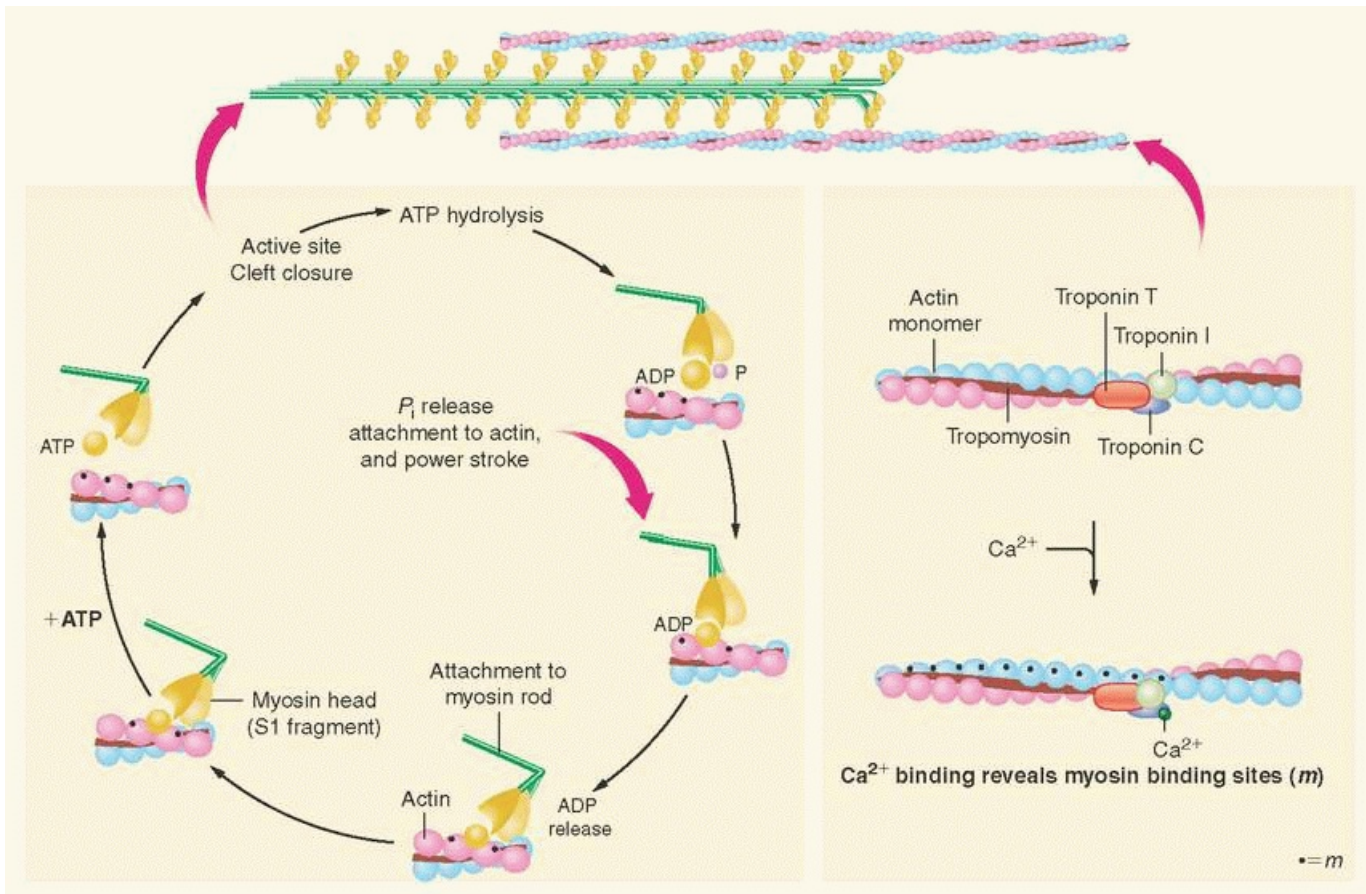


**Figure 12-8** Schematic illustration of the actin filaments and its individual monomers and active myosin-binding sites ( $m$ ; left panel). The myosin head is dissociated from actin by binding with adenosine triphosphate (ATP). Subsequent ATP hydrolysis and release of inorganic phosphate ( $P_i$ ) “cocks” the head group into a tension-generating configuration. Attachment of the myosin head to actin allows the head to apply tension to the myosin rod and the actin filament. The right panel illustrates  $Ca^{2+}$  binding to troponin C, which causes troponin I to decrease its affinity for actin. As a result in a conformational shift in tropomyosin position (see text), seven sites on actin monomers are revealed.

A  $Ca^{2+}$ -ATPase located in the SR membrane (**sarcoendoplasmic reticulum  $Ca^{2+}$ -ATPase, SERCA**) removes most of the  $Ca^{2+}$  ions from the myofilaments and the cytosol after membrane repolarization. This  $Ca^{2+}$  is stored (approximately  $10^{-3}$  M) in the SR bound to calsequestrin and calreticulin until the next sarcolemmal depolarization. The  $Na^+$ - $Ca^{2+}$  exchanger and a  $Ca^{2+}$ -ATPase located within the sarcolemmal membrane also remove a small quantity of  $Ca^{2+}$  from the sarcoplasm. Phospholamban is a small protein (6 kDa) located in the SR membrane that partially inhibits the activity of the dominant form (type 2a) of cardiac SERCA under baseline conditions. However, phosphorylation of this protein by protein kinase A blocks this inhibition and enhances the rate of SERCA uptake of  $Ca^{2+}$  into the SR.<sup>23</sup> This action increases the rate and extent of relaxation (positive lusitropic effect) and augments the amount of  $Ca^{2+}$  available for the next contraction (positive inotropic effect). Thus, a cAMP-dependent protein kinase that is responsive to  $\beta_1$  adrenoceptor stimulation or phosphodiesterase fraction III inhibition regulates SERCA activity. This observation explains why positive inotropic drugs such as dobutamine and milrinone also augment relaxation.

### **Myosin-Actin Interaction**

The biochemistry of sarcomere contraction is most often described using a simplified four-component model (Fig. 12-8).<sup>24</sup> High-affinity binding of ATP to the catalytic domain of myosin initiates the series of events that cause



sarcomere contraction. Myosin ATPase hydrolyzes the ATP molecule into ADP and inorganic phosphate, but the reaction products do not immediately dissociate from myosin. Instead, an “active” complex is

P.286

formed that retains the reaction's chemical energy as potential energy. In the absence of actin, subsequent dissociation of ADP and phosphate from myosin is the rate-limiting step of myosin ATPase. The muscle remains relaxed under these conditions. However, the activity of myosin ATPase is markedly increased when the myosin-ADP-phosphate complex is bound to actin, and the chemical energy obtained from ATP hydrolysis is transferred into mechanical work. Attachment of myosin to its binding site on the actin molecule releases the phosphate anion from the myosin head, producing a unique molecular conformation within the cross-bridge structure that generates tension in both myofilaments.<sup>25</sup> Release of ADP and the stored potential energy from this activated conformation produce rotation of the crossbridge (power stroke) at the hinge point separating the myosin helical tail region from the globular myosin head and its associated light chain proteins. Each cross-bridge rotation generates 3 to  $4 \times 10^{-12}$  N of force and moves myosin 11 nm along the actin molecule.<sup>26</sup> Completion of myosin head rotation and ADP release does not immediately dissociate the myosin-active complex, but leaves it in a low-energy bound (rigor) state. Separation of myosin and actin requires binding of a new ATP molecule to myosin. The process is then repeated, provided that there is an adequate ATP supply and troponin-tropomyosin inhibition does not block the myosin-binding site on actin.

Several factors may affect the efficiency of cross-bridge biochemistry and myocardial contractility independent of autonomic nervous system activity or administration of vasoactive drugs. A direct relationship between myosin ATPase activity and the maximal velocity of unloaded muscle shortening ( $V_{max}$ ) exists. The normal increase in intracellular  $Ca^{2+}$  concentration that occurs after sarcolemmal depolarization (from  $10^{-7}$  to  $10^{-5}$  M) enhances baseline myosin ATPase activity fivefold before it interacts with actin, increasing  $V_{max}$ . Contractile force also depends on sarcomere length immediately before sarcolemmal depolarization. This length-dependent activation (Frank-Starling effect) may be related to an increase in myofilament  $Ca^{2+}$  sensitivity, favorable alterations in spacing between myofilaments, or titin-induced elastic recoil. An abrupt increase in load during contraction (Anrep effect) or after a prolonged pause between beats (Woodworth phenomenon) transiently enhances contractile force through a length-dependent activation mechanism. Increased myofilament  $Ca^{2+}$  sensitivity and greater SR  $Ca^{2+}$  release are the putative mechanisms responsible for the positive inotropic effect of faster cardiac myocyte stimulation frequency (Treppe phenomenon; see below).

## Law of Laplace

  The Law of Laplace allows translation of changes in tension and length observed in the cardiac myocyte into alterations in pressure and volume that occur in the intact heart.<sup>27</sup> A pressurized, spherical shell is a simple model for relating cardiac myocyte tension and length to LV pressure and volume (Fig. 12-9). The geometry of the LV more closely resembles a prolate ellipsoid,<sup>28</sup> but a pressurized sphere is quite useful for the purposes of the current discussion. Tension development in each myocyte increases LV wall stress ( $\sigma$ ; tension exerted over a cross-sectional area) that is transformed into pressure ( $p$ ) when applied to a fluid (blood). Three assumptions are used in this derivation of the Law of Laplace: first, the LV is spherical in shape with an internal radius ( $r$ ) and uniform wall thickness ( $h$ ); second,  $\sigma$  is presumed to be constant throughout the thickness of the LV wall; and third, the LV exists in static equilibrium (i.e., is not actively contracting). In this model, “ $p$ ” is the force acting to distend the LV, whereas “ $\sigma$ ” represents the force resisting this distension. It can be easily shown that  $\sigma = pr/2h$ , indicating that wall stress varies directly with pressure and chamber radius and inversely with wall thickness. Despite the model's assumptions and simplicity, this version of the Law of Laplace allows appreciation

of the factors that alter LV wall stress and how cardiac pathology influences them. For example, the chronically elevated LV pressure ( $p$ ) that occurs in the presence of severe aortic valve stenosis or uncontrolled essential hypertension increases  $\sigma$  because these variables are directly related. Similarly, LV dilation associated with chronic mitral regurgitation also increases  $\sigma$  because the internal diameter ( $r$ ) of the LV is larger. Notably, increases in wall stress in either of these circumstances causes greater myocardial oxygen consumption because each myocyte uses more energy when developing greater tension.<sup>29</sup> Conversely, an increase in wall thickness ( $h$ ) decreases  $\sigma$ . This observation emphasizes that hypertrophy is an essential compensatory response to elevated wall stress that reduces the developed tension in each myocyte. More complete descriptions of the Law of Laplace have been derived in which more anatomically realistic LV geometry and wall stress are used, but the fundamental principles relating wall stress to pressure, radius, and wall thickness remain essential elements in these models.<sup>30,31</sup>

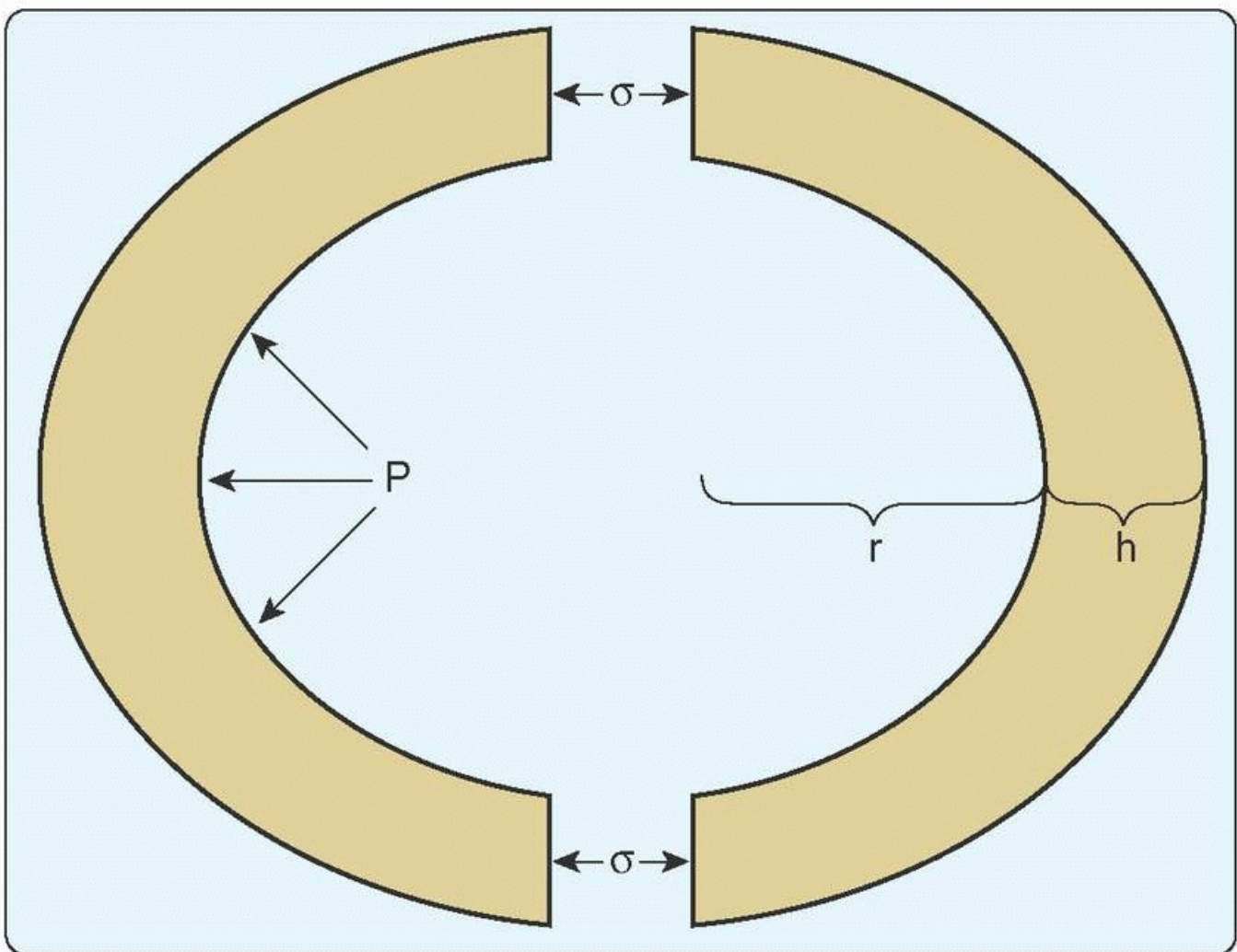


**Figure 12-9** This schematic diagram depicts the opposing forces within a theoretical LV sphere that determine the Law of Laplace. LV pressure ( $P$ ) pushes the sphere apart, whereas wall stress ( $\sigma$ ) holds the sphere together.  $r$ , LV radius;  $h$ , LV thickness. (Reproduced with permission from Kaplan JA, Reich DL, Savino JS. *Kaplan's Cardiac Anesthesia: The Echo Era*. 6th ed. St. Louis, MO: Elsevier Saunders; 2011:105.)

## The Cardiac Cycle

The temporal relationship between the electrical, mechanical, and valvular events that occur during the cardiac cycle<sup>32</sup> are illustrated in Figure 12-10. The QRS complex of the electrocardiogram indicates that RV and LV depolarization has occurred. This electrical activation initiates contraction (systole) and is associated with rapid

increases in pressure in both chambers ( $LV > RV$ ). When RV and LV pressures are greater than RA and LA pressures, the tricuspid and mitral valves close, respectively, and produce first heart sound ( $S_1$ ). Isovolumic contraction, rapid ejection, and slower ejection phases are the three major phases of LV systole. During LV isovolumic contraction, LV volume is constant because both the aortic and mitral valves are closed.

P.287

However, LV shape becomes more spherical because of decreases in longitudinal dimension. The maximal rate of increase in LV pressure ( $+dP/dt$ ), a commonly used index of myocardial contractility, also occurs during LV isovolumic contraction. In contrast to the synchronous LV, the peristaltic-like contraction of the RV inflow and outflow tracts precludes true isovolumic contraction in the RV.<sup>33, 34</sup> The pressures in the aortic and pulmonic roots reach their minima before the corresponding valves open. When LV and RV pressures are greater than aortic and PA pressures, respectively, rapid ejection of approximately two-thirds of the end-diastolic volume of each chamber occurs. The kinetic energy of LV and RV contraction is stored as potential energy in the elastic aorta and PA, respectively, which is then released to the corresponding distal vascular beds during diastole. The relative compliance of the proximal systemic and PA vasculature determines the magnitude of this stored potential energy. As aortic and PA pressures reach their maximum values, ejection falls dramatically and stops entirely when the ventricles begin to repolarize. Aortic and PA pressures briefly exceed LV and RV pressures as this slower ejection phase comes to an end, and the corresponding valves close in response to these reversed pressure gradients. Valve closure causes the second heart sound ( $S_2$ ); this event denotes end-systole.  $S_2$  is normally split because the pulmonic valve closes slightly after the aortic valve.

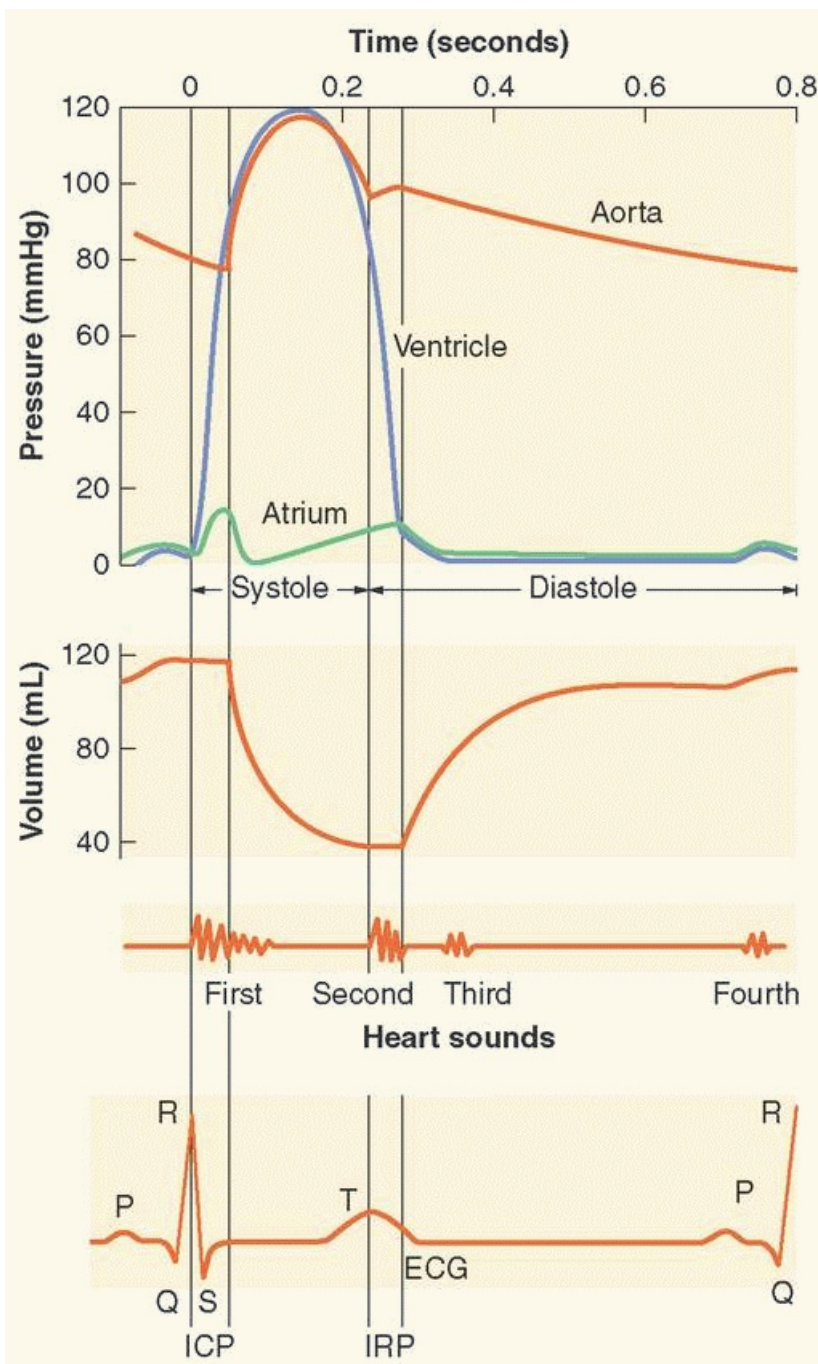



**Figure 12-10** Mechanical and electrical events of the cardiac cycle showing also the LV volume curve and the heart sounds. Note the LV isovolumic contraction (ICP) and the relaxation period (IRP), during which there is no change in LV volume because aortic and mitral valves are closed. The LV decreases in volume as it ejects its contents into the aorta. During the first third of systolic ejection (the rapid ejection period), the curve of emptying is steep. ECG, electrocardiogram.

Isovolumic relaxation, early ventricular filling, diastasis, and atrial systole are the four phases of LV diastole. LV volume is constant during isovolumic relaxation because both the aortic and mitral valves are closed. LV pressure very rapidly declines as the myofilaments uncouple. The mitral valve opens when LA pressure exceeds LV pressure, and the pressure gradient between the chambers drives blood stored in the LA into the LV. LV pressure continues to fall after the mitral valve opens<sup>35</sup> because sarcomere relaxation is incomplete and recoil of compressed elastic components occurs. This process establishes a time-dependent pressure gradient between the LA and LV.<sup>36</sup> The instantaneous LA pressure immediately before mitral valve opening combined with the rate and extent with which LV pressure declines are the primary determinants of the pressure gradient between the two chambers.<sup>37</sup> Early LV filling is quite rapid: the peak velocities of mitral blood flow during early filling and

aortic blood flow during ejection are similar (approximately 1 m/s).<sup>38</sup> Transmitral blood flow causes a vortex ring to form within the LV, which facilitates selective filling of the LV outflow tract because of the LV's structural asymmetry.<sup>39</sup> Age and cardiac disease (e.g., myocardial ischemia, pressure-overload hypertrophy) often delay LV relaxation, an important cause of diastolic dysfunction because the LA-to-LV pressure gradient is reduced, early LV filling is attenuated, and vortex ring formation is partially inhibited.<sup>40, 41</sup> LV pressure will continue to fall to subatmospheric values if blood flow across the mitral valve is experimentally prevented.<sup>42</sup> This “diastolic suction” effect assures that the LV continues to fill even if LA pressure is zero (e.g., during profound hypovolemia or intense exercise).<sup>43</sup> The early filling phase of diastole normally provides 70% to 75% of final stroke volume. During the third phase of diastole, the LA acts as a conduit for pulmonary venous blood flow to flow freely through the open mitral valve into the LV. Less than 5% of total stroke volume enters the LV during diastasis, which may be shortened or eliminated by tachycardia.<sup>44</sup> The final phase of diastole is atrial systole. LA contraction again creates a positive pressure LA to LV gradient and stimulates active blood flow. The sphincter-like anatomy of the pulmonary venous-LA junction largely prevents retrograde blood flow into the pulmonary veins unless LA pressure is markedly elevated (e.g., heart failure, severe mitral regurgitation). Atrial systole normally generates 15% to 25% of final stroke volume, but this percentage increases when delayed LV relaxation or reduced LV compliance is present. Thus, it is common for patients with such abnormalities to develop acute hemodynamic instability when LA contraction suddenly becomes timed improperly (e.g., AV conduction block) or disappears entirely (e.g., atrial fibrillation).

Three major deflections are observed in the LA pressure waveform during sinus rhythm. LA contraction follows the P wave of atrial depolarization and produces the “a” wave of atrial systole. An increase in LA preload or contractility augments the magnitude of the “a” wave. The rate of deceleration of the “a” wave is an index of LA relaxation.<sup>45</sup> A second small increase in LA pressure occurs with the onset of LV contraction because the mitral valve closes. This deflection is known as the “c” wave. The final “v” wave results from LA filling during LV systole and early relaxation as pulmonary venous return enters the LA while the mitral valve is closed. Mitral regurgitation or reduction in LA compliance enhances the magnitude of this “v” wave.<sup>46</sup> Similar changes in the RA pressure waveform deflections also occur. Indeed, the RA “a-c-v” morphology is easily observed in the external jugular veins when examining most patients in supine position.

## The Pressure-Volume Diagram

**4**  A simultaneous temporal plot of continuous LV pressure and volume creates a phase-space diagram that is useful for analysis of LV systolic and diastolic function (Fig. 12-11). The LV pressure-volume (P-V) diagram proceeds in a counterclockwise direction. End-diastole initiates the cardiac cycle (point A, Fig. 12-11). This is followed by isovolumic contraction, in which a rapid increase in LV pressure occurs without change in LV volume. When LV pressure is greater than aorta pressure, the aortic valve opens (point B, Fig. 12-11). Ejection of blood from the LV volume into the aorta and the proximal great vessels causes a precipitous decline in LV volume. The aortic valve closes when LV pressure drops below aortic pressure (point C, Fig. 12-11). When LV pressure falls below LA pressure during isovolumic relaxation, the mitral valve opens (point D, Fig. 12-11) and LV filling then occurs, causing a large increase in LV volume concomitant with a small increase in LV pressure during the remainder of diastole. This final stage completes a single circuit (cardiac cycle) around the P-V diagram.

**5** The LV P-V diagram allows recognition of major cardiac events (e.g., aortic and mitral valve opening and closing) without formal electrocardiographic correlation. The lower right and upper left corners of the P-V

diagram identify the LV end-diastolic and endsystolic volumes (EDV and ESV, respectively), which facilitate calculation of stroke volume (SV; EDV - ESV) and ejection fraction (EF; SV/EDV). The normal EDV and ESV are approximately 120 and 40 mL, respectively. Thus, SV is 80 mL and EF is 67%. The area of the LV P-V diagram defines stroke work for the cardiac cycle. An increase in preload is indicated by a rightward shift of the right side of the LV P-V diagram. Elevated height (greater LV systolic pressure) and a narrower width (reduced SV) of the LV P-V diagram indicates the presence of increased afterload. A series of LV P-V diagrams may be acquired as a result of an acute change in LV loading conditions over several cardiac cycles and is useful for determining contractile state, chamber compliance, and mechanical efficiency. Changes in preload or afterload may be produced mechanically (e.g., transient inferior vena caval or proximal aortic occlusion) or pharmacologically (e.g., intravenous infusion of nitroglycerin or phenylephrine) to generate a nested set of differentially loaded LV P-V diagrams. These loops may then be used to determine the end-systolic pressure-volume relation (ESPVR), the slope of which ("end-systolic elastance" [ $E_{es}$ ]) is a relatively heart-rate- and load-independent index of myocardial contractility in vivo.<sup>47</sup> The same set of LV P-V diagrams may also be used to calculate the end-diastolic pressure-volume relationship (EDPVR) and quantify LV compliance.<sup>27</sup> The ESPVR and EDPVR establish the operational range of the LV and define the LV's mechanical characteristics during systole and diastole, respectively.<sup>48</sup> The triangular space that lies between ESPVR and EDPVR to the left of the steady-state LV P-V diagram is the potential energy remaining in the system and is often used to quantify the LV's energetics and mechanical efficiency.<sup>49</sup> The principles of pressure-volume analysis have also been successfully applied to the study of RV and LA function.<sup>50 51</sup>

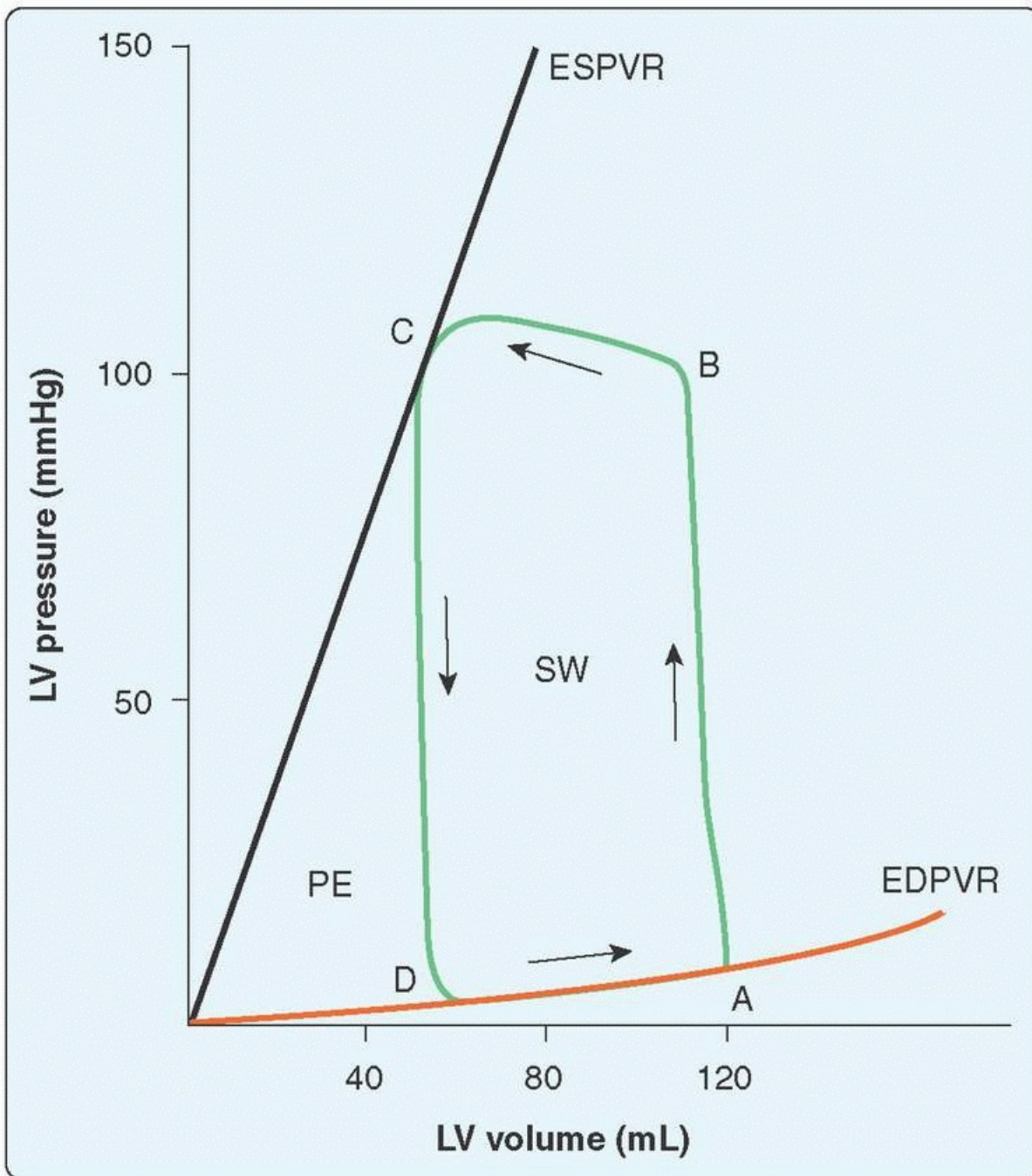


**Figure 12-11** This illustration depicts the steady-state LV pressure-volume diagram. The cardiac cycle proceeds in a time-dependent counterclockwise direction (*arrows*). Points A, B, C, and D correspond to LV end-diastole (closure of the mitral valve), opening of the aortic valve, LV end-systole (closure of the aortic valve), and opening of the mitral valve, respectively. Segments AB, BC, CD, and DA represent isovolumic contraction, ejection, isovolumic relaxation, and filling, respectively. The LV is constrained to operate within the boundaries of the end-systolic and end-diastolic pressure-volume relations (ESPVR and EDPVR, respectively). The area inscribed by the LV pressure-volume diagram is stroke work (SW) performed during the cardiac cycle. The area to the left of the LV pressure-volume diagram between ESPVR and EDPVR is the remaining potential energy (PE) of the system. (Reproduced with permission from Kaplan JA, Reich DL, Savino JS. *Kaplan's Cardiac Anesthesia: The Echo Era*. 6th ed. St. Louis, MO: Elsevier Saunders; 2011:107.)

LV systolic or diastolic heart failure may be clearly depicted using P-V analysis.<sup>52</sup> Pure LV systolic dysfunction is represented by a reduction in the ESPVR slope and often occurs in conjunction with LV dilation, as illustrated by a right shift of the P-V diagram without a substantial change in the position of EDPVR (Fig. 12-12). The increase in preload (right shift) is a compensatory response to depression of myocardial contractility that serves to



maintain stroke volume, but occurs at a cost of elevated LV filling pressure, greater LV volume, and increased myocardial oxygen consumption. An increase in EDPVR defines a reduction in LV compliance consistent with LV diastolic dysfunction because LV pressure is greater for a given LV volume. In pure diastolic heart failure, myocardial contractility is preserved (ESPVR is unchanged), but clinical symptoms are present because LV filling pressures are elevated. Simultaneously depressed ESPVR and elevated EDPVR are observed in the presence of combined LV systolic and diastolic dysfunction. Under these circumstances, the LV operates in a restricted range of preload and afterload conditions. Stroke volume and cardiac output are often substantially compromised as a result, leading to global tissue malperfusion.

## Determinants of Systolic Function

**6** The LV's ability to collect and eject blood determines its overall performance. The amount of blood that the LV contains before the onset of contraction (preload), the arterial resistance to emptying that the LV must overcome during ejection (afterload), and the contractile properties of the LV myocardium (inotropic state) determine the stroke volume for each cardiac cycle (Fig. 12-13). These three factors combine with the heart rate and rhythm to

P.289

determine cardiac output. The LV's structural integrity is essential to its efficiency as a pump. For example, an anomalous route of blood flow from the chamber (e.g., a ventricular septal defect with left to right shunt) or valvular dysfunction (e.g., severe mitral regurgitation) may reduce forward flow because blood is diverted into lower pressure outlets (the RV or the LA in these examples, respectively) and is not ejected directly into the aorta. Pulmonary venous blood flow, LA and mitral valve function, pericardial forces, and the active (relaxation) and passive (compliance) diastolic properties of the LV determine the LV's ability to fill properly at normal pressure (approximately 10 mmHg).<sup>53</sup> Perturbations in any of these variables attenuates optimal LV filling and may contribute to the development of heart failure independent of LV systolic dysfunction per se.

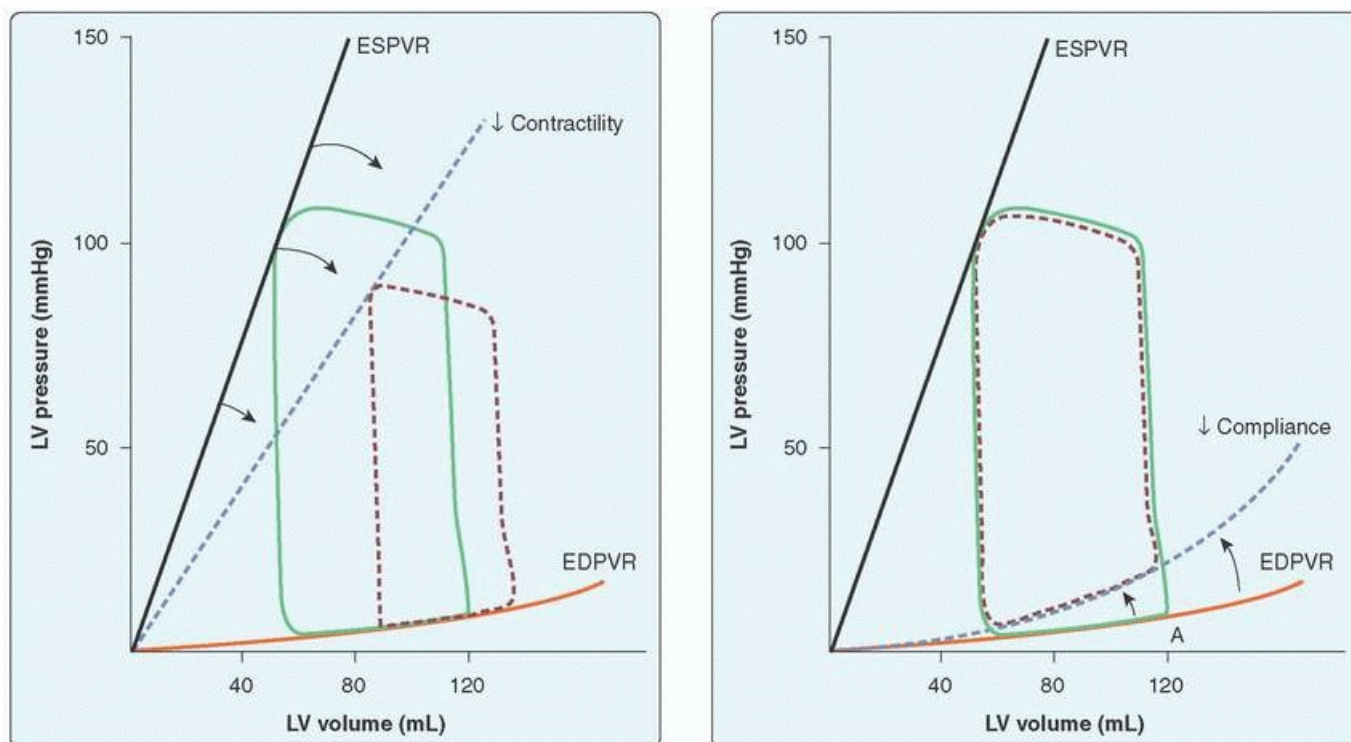


**Figure 12-12** These schematic illustrations demonstrate alterations in the steady-state LV pressure-volume diagram produced by a reduction in myocardial contractility as indicated by a decrease in the slope of the end-systolic pressure-volume relation (ESPVR; left panel) and a decrease in LV compliance as indicated by an increase in the position of the end-diastolic pressure-volume relation (EDPVR; right panel). These diagrams

emphasize that heart failure may result from LV systolic or diastolic dysfunction independently. Reproduced with permission from Kaplan JA, Reich DL, Savino JS. *Kaplan's Cardiac Anesthesia: The Echo Era*. 6th ed. St. Louis, MO: Elsevier Saunders; 2011:109.)

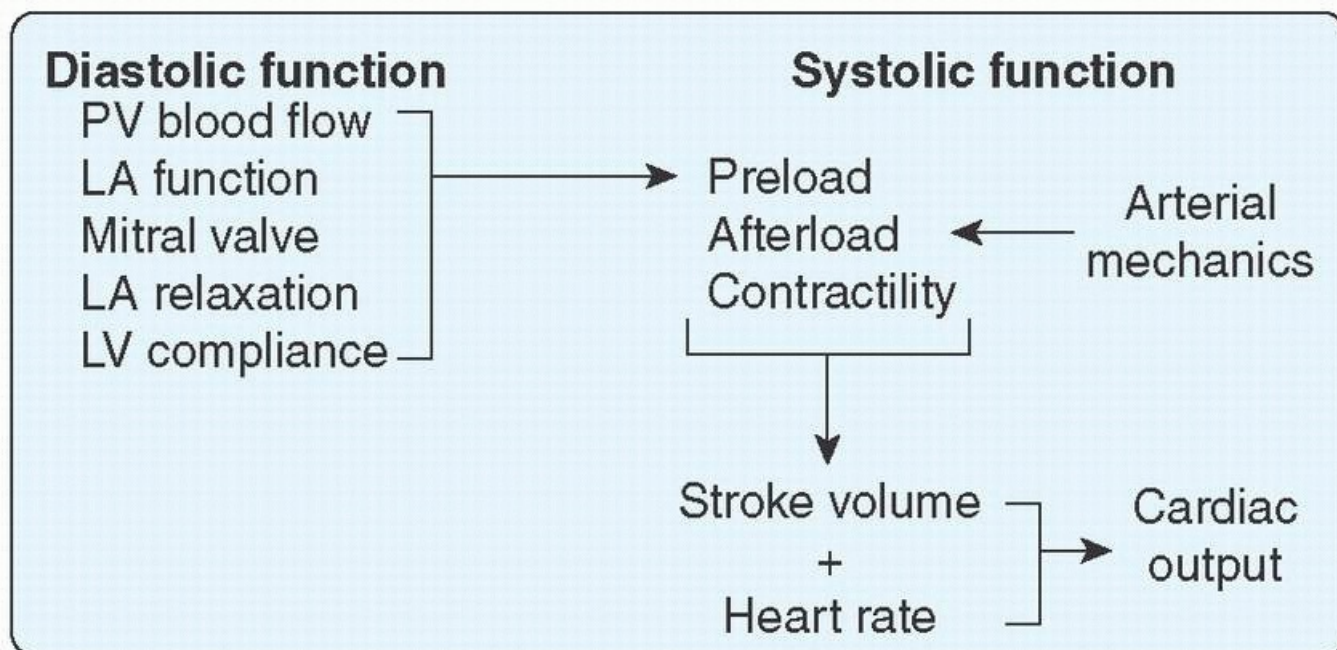


**Figure 12-13** This illustration depicts the major factors that determine LV diastolic (left) and systolic (right) function. Note that pulmonary venous (PV) blood flow, LA function, mitral valve integrity, LA relaxation, and LV compliance combine to determine LV preload. (Reproduced with permission from Kaplan JA, Reich DL, Savino JS. *Kaplan's Cardiac Anesthesia: The Echo Era*. 6th ed. St. Louis, MO: Elsevier Saunders; 2011:111.)

### Heart Rate

The contractile state of isolated cardiac muscle is directly related to its stimulation frequency. This phenomenon is known as the Bowditch, “staircase,” or “Treppe” effect, or the “force-frequency” relationship. Improved  $\text{Ca}^{2+}$  cycling efficiency and increased myofilament  $\text{Ca}^{2+}$  sensitivity are most likely responsible for the Bowditch effect. Maximal contractile force is generated at 150 to 180 stimulations/min in isolated cardiac muscle. These experimental data support the clinical observation of ideal matching of cardiac output to venous return at heart rates of approximately 175 beats/min during intense aerobic exercise in trained endurance athletes. Contractility begins to decrease at heart rates exceeding 175 beats/min because LV relaxation abnormalities begin to develop. Insufficient  $\text{Ca}^{2+}$  uptake from the contractile apparatus, attenuated LV diastolic filling time, and reduced coronary perfusion resulting from an inadequate duration of diastole combine to contribute to the reduction in inotropic state and cardiac output during profound tachycardia. Thus, tachyarrhythmias or rapid pacing may cause profound hemodynamic compromise, even in otherwise healthy individuals. The Bowditch effect is a particularly important mechanism by which contractility is enhanced and adequate arterial blood pressure is maintained in disease states characterized by profound impairments in LV filling (e.g., pericardial tamponade, constrictive pericarditis). The

P.290

“interval-strength” effect is another manifestation of the Bowditch phenomenon in which the force of LV contraction is augmented after an extrasystole.<sup>54</sup> Notably, the Bowditch effect is most likely of little consequence within a typical physiologic range of heart rate (e.g., 50 to 150 beats/min) in the normal heart.<sup>55</sup>

### Preload

**7** Sarcomere length in vitro immediately before myocyte contraction is a useful way to appreciate the concept of “preload,” but this microscopic definition is difficult to envision in vivo considering the LV’s complex three-dimensional structure. Instead, EDV is most often used to define LV preload because this volume of blood establishes the precontraction length of each LV sarcomere and is directly related to LV end-diastolic wall stress. Real-time quantification of LV EDV continues to be quite challenging from a clinical perspective. Experimental methods used to measure LV EDV (e.g., sonomicrometry, conductance catheter technology) are very precise but impractical because they require invasive instrumentation.<sup>56,57</sup> Noninvasive methods, including radionuclide angiography or dynamic magnetic resonance imaging, may also be used to measure LV EDV, but these imaging techniques cannot be used in the operating room or intensive care unit. Three-dimensional transesophageal echocardiography (TEE) is increasingly used to provide real-time estimates of LV EDV and EF during surgery,<sup>58,59,60</sup> but this technique may be difficult to apply during rapidly changing hemodynamic conditions. Cardiac anesthesiologists often estimate LV EDV using two-dimensional TEE in the transgastric LV midpapillary short axis view to measure or visually estimate LV end-diastolic area or diameter. A decrease in LV preload is usually inferred when there is a reduction in end-diastolic area and diameter, although marked arterial vasodilation may also produce similar findings.

Other clinically used indices of LV preload have inherent limitations (Fig. 12-14). Advancing a fluid-filled catheter into the LV allows measurement of LV end-diastolic pressure, which is related to EDV through the exponential EDPVR curve. This invasive technique is possible only in the cardiac catheterization laboratory or the operating room. In lieu of this method, other pressures “upstream” from the LV are more commonly used to estimate LV EDV, including mean LA, pulmonary capillary occlusion (wedge), pulmonary arterial diastolic, RV enddiastolic, and RA (central venous) pressures. The integrity of the structures that separate each site of measurement from the LV influences the relative accuracy of these methods. For example, a correlation between central venous and LV end-diastolic pressures assumes that pulmonary disease, airway pressure during respiration, RV or pulmonary vascular disease, LA dysfunction, mitral valve abnormalities, or abnormal LV compliance have not adversely affected the fluid column between the RA and the LV. This is not the case in many patients with significant pulmonary or cardiac disease. For example, there is a well-known lack of correlation between LV EDV, pulmonary artery occlusion pressure, and central venous pressure in patients with LV dysfunction,<sup>61</sup> in whom accurate measurement of LV preload may be especially important to optimize hemodynamics.

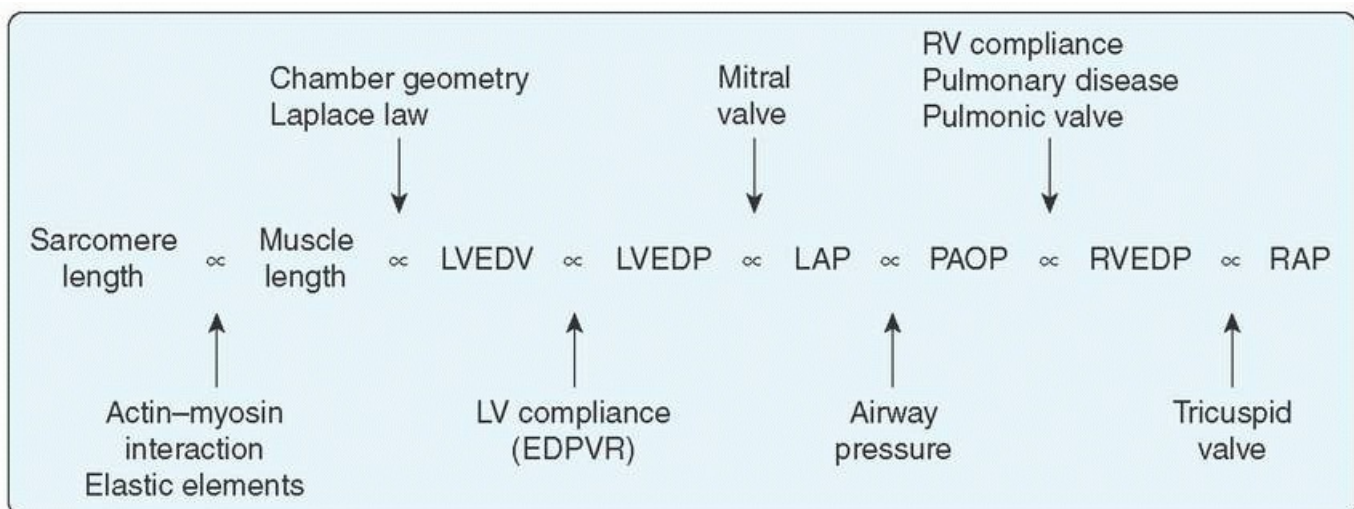


**Figure 12-14** This schematic diagram depicts factors that influence experimental and clinical estimates of sarcomere length as a pure index of the preload of the contracting LV myocyte. LVEDV and LVEDP, LV end-diastolic volume and end-diastolic pressure, respectively; EDPVR, end-diastolic pressure-volume relation; LAP, left atrial pressure; PAOP, pulmonary artery occlusion pressure; RV, right ventricle; RVEDP, RV end-diastolic

pressure; RAP, right atrial pressure. (Reproduced with permission from Kaplan JA, Reich DL, Savino JS. *Kaplan's Cardiac Anesthesia: The Echo Era*. 6th ed. St. Louis, MO: Elsevier Saunders; 2011:112.)

## Afterload

**8** The additional load to which cardiac muscle is exposed after contraction has begun is termed “afterload.” This concept is intuitively clear when studying isolated cardiac muscle under experimental conditions, but it is more difficult to quantify when the LV's interaction with the arterial vasculature is considered in vivo. Four components determine LV afterload in the intact cardiovascular system: the size and mechanical behavior of arterial blood vessels; terminal arteriolar vasomotor tone, which establishes total arterial resistance; LV end-systolic wall stress, which is defined by LV pressure development and the changes in LV geometry required to generate it; and the physical properties and volume of blood as a hydraulic fluid. This section will focus on LV afterload, but the methods used to estimate RV afterload are virtually identical to those used to quantify LV afterload.<sup>62</sup> Nevertheless, the reader should appreciate that two major differences exist between the LV and the RV afterload systems: the systemic circulation is substantially less compliant than pulmonary arterial vasculature and, as mentioned previously, the LV is less sensitive to changes in afterload than is the RV.

The most comprehensive description of LV afterload is aortic input impedance [ $Z_{in}(\omega)$ ], defined as the ratio of continuous aortic pressure (the forces acting on the blood) to blood flow (the motion that those forces creates). Power spectral or Fourier series analysis is used to calculate  $Z_{in}(\omega)$  from high-fidelity measurements of pressure and blood flow.  $Z_{in}(\omega)$  includes the frequency-dependent characteristics of the arterial vasculature, including its viscoelastic effects and wave reflection properties. This methodology is quite useful from a biomechanical engineering perspective, but has limited practical applicability. Another definition of LV afterload

P.291

quantifies the mechanical forces to which the LV is exposed at the end of ejection as LV end-systolic wall stress. As previously mentioned, a large decline in LV volume occurs after the aortic valve opens, concomitant with elevated LV pressure and increased wall thickness. The Law of Laplace indicates that changes in these variables cause a pronounced increase in LV end-systolic wall stress, which reaches its maximum value during early LV ejection and subsequently falls.<sup>28</sup> These alterations in LV systolic wall stress during ejection are important. Maximal LV systolic wall stress is a potent stimulus for myocyte hypertrophy in the presence of chronic increases in afterload, such as may be observed in patients with severe aortic valve stenosis or uncontrolled essential hypertension.<sup>63</sup> The area under the LV systolic wall stress curve is directly related to myocardial oxygen consumption.<sup>64</sup> At endsystole, the forces driving further ejection and those resisting it are equal. Thus, LV end-systolic wall stress is also a determinant of stroke volume.

Afterload may also be approached from a mechanical systems perspective, because the LV and the arterial vasculature must be appropriately matched to assure optimal energy transfer between them. In this “coupling” model, the LV and arterial circulation are considered elastic chambers in series. LV-arterial coupling is described using the ratio of LV elastance ( $E_{es}$ ) and effective arterial elastance ( $E_a$ ), each of which is determined in the P-V plane (Fig. 12-15).<sup>65</sup>  $E_a$  may also be estimated as the ratio of endsystolic arterial pressure to stroke volume, and has been clinically applied to approximate LV afterload using this definition. Arteriolar resistance and the compliance of the proximal great vessels influence  $E_a$ , but  $E_a$  does not include arterial frequency dependence or wave reflection properties and cannot be used as a quantitative index of LV afterload as a result.

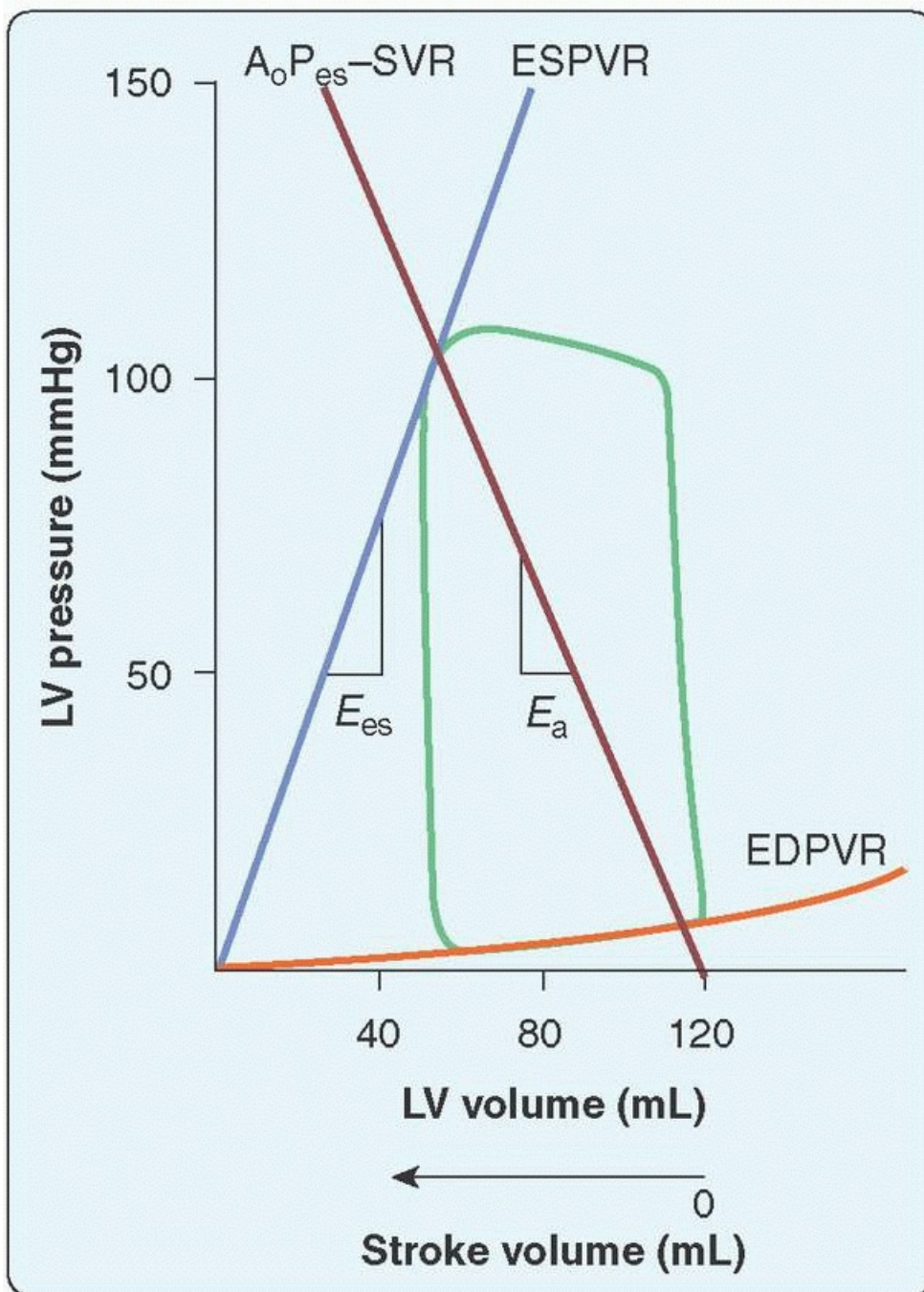


**Figure 12-15** This schematic diagram illustrates the LV end-systolic pressure-volume and aortic end-systolic pressure-stroke volume relations (ESPVR and  $A_0P_{es}$ -SVR, respectively) used to determine LV-arterial coupling as the ratio of end-systolic elastance ( $E_{es}$ ; the slope of ESPVR) and effective arterial elastance ( $E_a$ ; the slope of  $A_0P_{es}$ -SVR). EDPVR = end-diastolic pressure-volume relation. (Reproduced with permission from Kaplan JA, Reich DL, Savino JS. *Kaplan's Cardiac Anesthesia: The Echo Era*. 6th ed. St. Louis, MO: Elsevier Saunders; 2011:114.)

The most commonly used clinical estimate of LV afterload is systemic vascular resistance calculated as  $([MAP - RAP] \cdot 80)/CO$ , where MAP and RAP are mean arterial and right atrial pressures, respectively, CO is cardiac output, and 80 is a constant that converts  $\text{mmHg} \cdot \text{min}^{-1} \cdot \text{L}^{-1}$  to  $\text{dynes} \cdot \text{sec} \cdot \text{cm}^{-5}$ . Systemic vascular resistance primarily reflects the resistance of terminal arterioles, which is a major component of afterload. However, similar to LV end-systolic wall stress and  $E_a$ , systemic vascular resistance does not consider the mechanical properties of the blood and arterial walls, ignores the frequency-dependence of arterial pressure and blood flow, and does not account for arterial wave reflection. Notably, these components of LV afterload are of greater importance in



**Figure 12-16** LV pressure- and volume-overload produce compensatory responses based on the nature of the inciting stress. Wall thickening reduces (-) whereas chamber dilation increases (+) end-systolic wall stress as predicted by the Law of Laplace. LV pressure-overload hypertrophy has been linked to heart failure with normal ejection fraction (HFNEF), but LV volume-overload most often causes heart failure (HF) with reduced ejection fraction (EF). (Reproduced with permission from Kaplan JA, Reich DL, Savino JS. *Kaplan's Cardiac Anesthesia: The Echo Era*. 6th ed. St. Louis, MO: Elsevier Saunders; 2011:114.)

## Myocardial Contractility

**9** Myocardial contractility is the force that cardiac muscle is capable of producing during contraction under controlled loading conditions and stimulation rate. Determining myocardial contractility is relatively easy in isolated cardiac muscle, but this measurement is remarkably difficult in the intact heart. The ability to quantify inotropic state has important implications during the clinical management of patients with LV or RV contractile dysfunction, but a “gold standard” of myocardial contractility independent of heart rate and loading conditions remains elusive. Inotropic state and loading conditions are inextricably connected in the sarcomere<sup>69</sup> and thus, it is most likely not feasible to measure contractility as an independent variable. To date, indices derived from LV P-V analysis, isovolumic contraction, and ejection are the major approaches to the measurement of contractility in vivo, all of which have limitations.

The ratio of continuous LV pressure-to-volume during the cardiac cycle is termed “time-varying elastance”  $[E(t)]$ , such that  $E(t) = P(t)/[V(t) - V_0]$ , where  $P(t)$  and  $V(t)$  are the time-dependent changes in LV pressure and volume, respectively, and  $V_0$  is LV volume at zero mmHg of LV pressure.<sup>70</sup> In this model, maximum LV elastance ( $E_{max}$ ) occurs at or very close to the left upper corner of the steady-state LV P-V diagram. As mentioned previously, a nested set of LV P-V diagrams may be generated by an acute change in loading conditions; each loop in this set has a distinct  $E_{max}$ . These  $E_{max}$  values are linearly related and establish the ESPVR (Fig. 12-17). The slope of ESPVR (end-systolic elastance;  $E_{es}$ ) is an afterload-insensitive index of contractility because the analysis from which it is derived is performed at endsystole. Alterations in contractile state are reflected in changes in  $E_{es}$ . For example, dobutamine increases  $E_{es}$ , and the magnitude of this increase quantifies the positive inotropic effect of the drug. Another contractile index based on the Frank-Starling principle relating preload to cardiac output may also be derived from the same series of LV P-V diagrams. The area of each LV P-V diagram (stroke work; SW) in this nested set of loops and its corresponding EDV are linearly related, such that  $SW = M_{sw} \cdot (EDV - V_{sw})$ , where  $M_{sw}$  and  $V_{sw}$  are the slope and volume intercept of the relation. The slope of this “preload recruitable stroke work” relation has been shown to quantify changes in contractility in a relatively load-independent manner.<sup>71</sup>  $E_{es}$  and  $M_{sw}$  are not used on a routine basis in clinical anesthesiology because invasive measurement of LV pressure and volume is generally required for their derivation, and extensive offline analysis must be performed. Nevertheless, both indices of inotropic state are useful conceptual tools with which to understand LV, RV, and atrial contractility in the intact heart.

Indices of global myocardial contractility may also be derived during isovolumic contraction using the LV pressure waveform. The most commonly used isovolumic index of contractility is  $dP/dt$ . This index requires invasive measurement of continuous LV pressure and is most often recorded in the cardiac catheterization laboratory, but may also be estimated noninvasively using TEE.<sup>72</sup> LV  $+dP/dt$  sensitively indicates changes in contractile state, but its absolute value is less important than the magnitude of its change in response to an intervention such as administration of an inotropic drug (e.g., epinephrine). LV  $+dP/dt$  is generally considered to be afterload-independent because the aortic valve opens after the maximal rate of rise of LV pressure occurs. However,

+dP/dt is highly dependent on preload, and another index of contractility based on LV P-V analysis that accounts for this preload dependence has been developed and applied in laboratory and clinical settings.<sup>73</sup> LV mass, chamber geometry, and valve disease also influence +dP/dt. Decreases in global LV inotropic state caused by regional myocardial ischemia may also not be accurately quantified with +dP/dt, because compensatory increases in contractility occur in the surrounding nonischemic myocardium, thereby effectively normalizing overall function. Other isovolumic indices of contractility based on +dP/dt, including the rate

P.293

of rise of LV pressure at a predetermined LV pressure (e.g., dP/dt measured at 40 mmHg) or the ratio of dP/dt to maximum LV pressure (dP/dt/P) have also been used, but these measures do not provide unique information compared with +dP/dt.

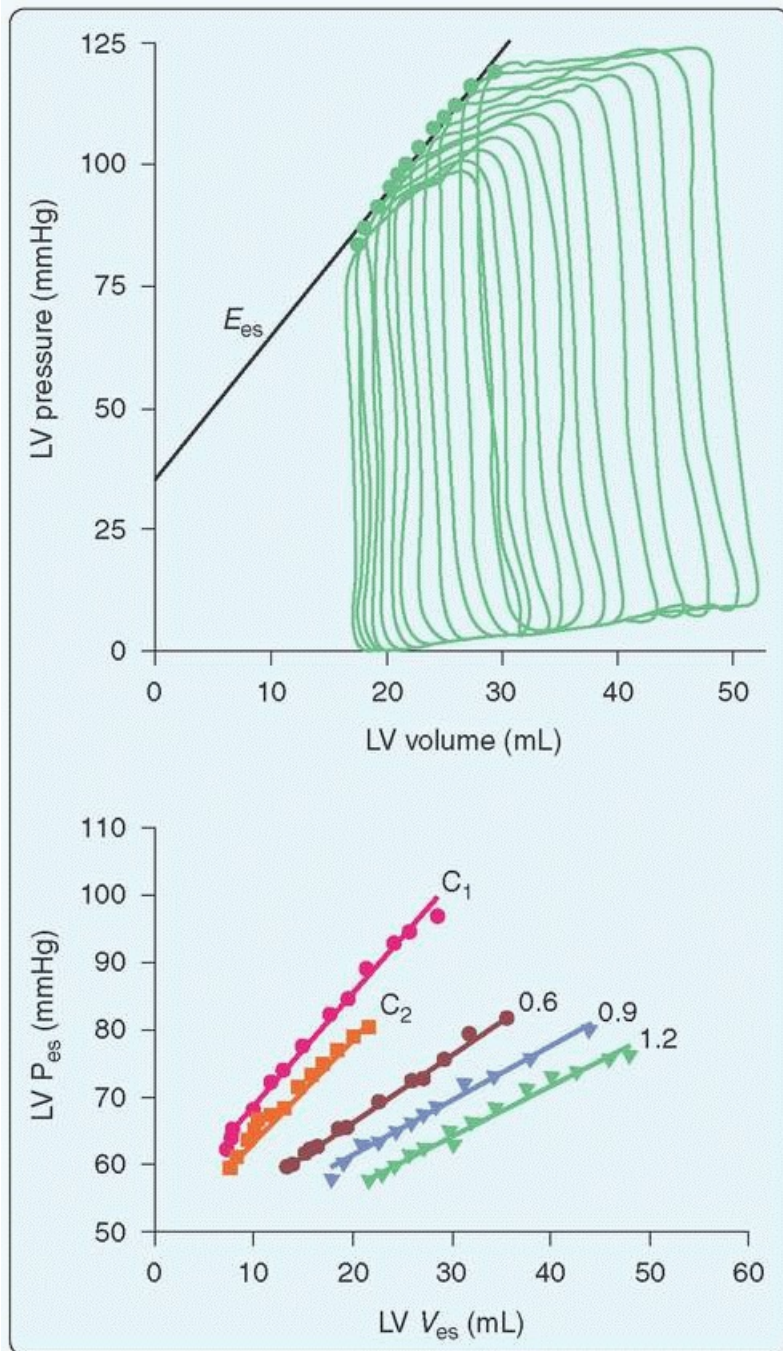


**Figure 12-17** This illustration depicts the method used to derive the LV end-systolic pressure-volume relation (ESPVR) from a series of differentially loaded LV pressure-volume diagrams generated by abrupt occlusion of the inferior vena cava in a canine heart *in vivo*. The maximal elastance ( $E_{max}$ ; pressure/volume ratio) for each pressure-volume diagram is identified as its left upper corner, and a linear regression analysis is used to define



the slope ( $E_{es}$ ; end-systolic elastance) and volume intercept of the ESPVR (top panel). The effects of isoflurane (0.6, 0.9, and 1.2 minimum alveolar concentration) on the ESPVR are illustrated in the bottom panel. C<sub>1</sub>, control 1 (before isoflurane); C<sub>2</sub>, control 2 (after isoflurane). (Reproduced with permission from Kaplan JA, Reich DL, Savino JS. *Kaplan's Cardiac Anesthesia: The Echo Era*. 6th ed. St. Louis, MO: Elsevier Saunders; 2011:116.)

Ejection fraction is the most commonly used clinical index of LV contractility. Ejection fraction is usually measured with two- or three-dimensional echocardiography, but other methods, including radionuclide angiography and magnetic resonance imaging (MRI), also provide reliable estimates of this ejection phase index of inotropic state. In the operating room, two-dimensional TEE midesophageal four- or two-chamber windows can be obtained at end-systole and end-diastole and analyzed using Simpson's rule of discs to determine EF. However, this technique is rather time-consuming and is impractical when hemodynamics are unstable. Instead, regional approximations of EF, such as fractional shortening and fractional area change (FAC), are often used by examining midpapillary short-axis diameter and area, respectively, at end-systole and end-diastole. For example, FAC is determined as  $EDA - ESA/EDA$ , where EDA and ESA are end-diastolic and end-systolic areas, respectively, measured by tracing the LV's endocardial borders (Fig. 12-18). All ejection phase indices of contractility are dependent on loading conditions and inotropic state. Thus, interpretation of EF, FAC, or fractional shortening must be considered within the clinical context under which the data were obtained. For example, profoundly depressed EF in a patient with severe hypertension may occur because afterload is markedly increased, and not because myocardial contractility is grossly impaired. Ejection phase indices may also be inaccurate in the presence of mitral or aortic valve disease or a ventricular septal defect. Indeed, EF may be greater than normal during acute mitral regurgitation because a substantial portion of blood flow from the LV is diverted into the LA during systole and not because the LV is inherently "hyperdynamic."

## Determinants of Diastolic Function

**10 11 12** Each chamber of the heart must fill adequately under normal pressures to facilitate optimal function during the subsequent contraction. We will emphasize LV diastolic function in the current section of this chapter, but the readers should be aware that the diastolic properties of the RV and atria are also important for the heart's overall performance. Because diastole is an inherently complex sequence of temporally related events (Table 12-1), no single index of LV diastolic function completely characterizes this phase of the cardiac cycle or selectively predicts those patients who may be at greatest risk of developing heart failure related to abnormal diastolic function.<sup>74</sup> Notably, nearly one-half of patients with heart failure do not have overt evidence of LV systolic dysfunction (e.g., a reduction in LV EF).<sup>75</sup> Hypertensive elderly women who are obese and have renal insufficiency, anemia, or atrial fibrillation appear to be at greatest risk of developing this "heart failure with normal ejection fraction" (HFNEF; also known as "diastolic heart failure").<sup>76</sup> Delayed LV relaxation, reduced compliance, and abnormal LV-arterial coupling have been implicated in the pathophysiology of HFNEF

P.294

(Table 12-1).<sup>77, 78</sup> Thus, LV diastolic dysfunction is a major cause of HFNEF. The severity of and response to medical therapy in HFNEF are key factors that establish exercise tolerance<sup>79</sup> and predict prognosis.<sup>80</sup> From the anesthesiologist's perspective, LV diastolic function is a major determinant of the LV's response to changes in loading conditions. Many volatile and intravenous anesthetics affect LV relaxation and filling in the normal and failing heart.<sup>81</sup> As a result, preoperative determination of the presence, severity, and underlying etiology of LV diastolic dysfunction (Table 12-2) is important when caring for patients undergoing surgery in which large shifts in intravascular volume are anticipated. Isolated LV diastolic dysfunction is also an independent risk factor for adverse cardiovascular events, including mortality, in patients undergoing major surgery.<sup>82</sup>

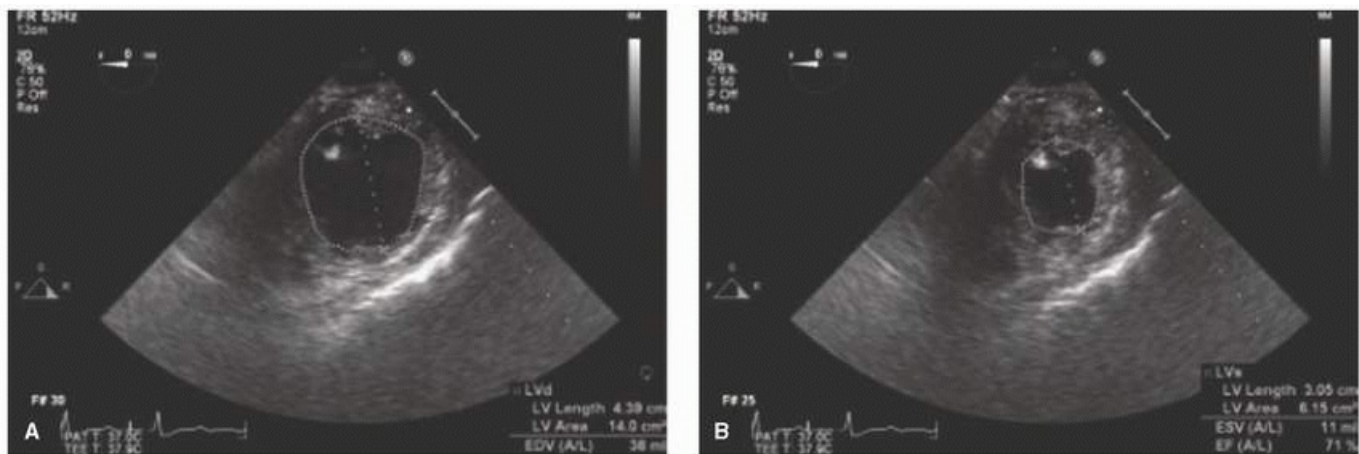


**Figure 12-18** Calculation of fractional area change from LV midpapillary short axis images obtained at end-diastole (left panel) and end-systole (right panel). The LV endocardial border is manually traced (excluding the papillary muscles). The software integrates the area inscribed in the LV chamber. (Reproduced with permission from Kaplan JA, Reich DL, Savino JS. *Kaplan's Cardiac Anesthesia: The Echo Era*. 6th ed. St. Louis, MO: Elsevier Saunders; 2011:119.)

**Table 12-1 Determinants of Left Ventricular Diastolic Function**

Heart rate and rhythm
LV systolic function
Wall thickness
Chamber geometry
Duration, rate, and extent of myocyte relaxation
LV untwisting and elastic recoil
Magnitude of diastolic suction
LA-LV pressure gradient
Passive elastic properties of LV myocardium
Viscoelastic effects (rapid LV filling and atrial systole)
LA structure and function
Mitral valve structure and function
Pulmonary venous blood flow

Pericardial restraint

RV loading conditions and function

Ventricular interdependence

Coronary blood flow and vascular engorgement

Compression by mediastinal masses

---

LV, left ventricle; LA, left atrium; RV, right ventricle.

Reprinted with permission from Kaplan JA, Reich DL, Savino JS. *Kaplan's Cardiac Anesthesia: The Echo Era*. 6th ed. St. Louis, MO: Elsevier Saunders; 2011:121.

### **Table 12-2 Common Causes of Left Ventricular Diastolic Dysfunction**

---

Age > 60 years

Acute myocardial ischemia (supply or demand)

Myocardial stunning, hibernation, or infarction

Ventricular remodeling after infarction

Pressure-overload hypertrophy (e.g., aortic stenosis, hypertension)

Volume-overload hypertrophy (e.g., aortic or mitral regurgitation)

Hypertrophic obstructive cardiomyopathy

Dilated cardiomyopathy

Restrictive cardiomyopathy (e.g., amyloidosis, hemochromatosis)

Pericardial diseases (e.g., tamponade, constrictive pericarditis)

---

Reprinted with permission from Kaplan JA, Reich DL, Savino JS. *Kaplan's Cardiac Anesthesia: The Echo Era*. 6th ed. St. Louis, MO: Elsevier Saunders; 2011:121.

### ***Invasive Assessment of LV Relaxation***

Removal of  $\text{Ca}^{2+}$  from the contractile apparatus and the sarcoplasm is an active, energy-dependent process that results in rapid dissociation of contractile proteins and recoil of compressed elastic elements. Failure of actin-myosin cross bridges to properly dissociate or abnormal removal of intracellular  $\text{Ca}^{2+}$  delays relaxation in the intact LV.<sup>83</sup> As mentioned previously, early LV filling is dependent on the rate and extent of LV relaxation and thus, is attenuated when relaxation is delayed. Under these circumstances, final EDV becomes more dependent on the contribution of atrial systole. As a result, acute onset of atrial fibrillation often causes heart failure in patients with disease states in which pronounced delays in LV relaxation occur (e.g., hypertrophic cardiomyopathy). Myocardial ischemia caused by acute occlusion of a major coronary artery is also a frequent cause of delayed LV relaxation and may be accompanied by reductions in LV compliance that further limit LV filling, cause LA and pulmonary venous hypertension, and contribute to the development of pulmonary edema.<sup>84</sup>

Measuring the rate with which LV pressure declines during isovolumic relaxation is the most common technique for quantifying LV relaxation. This type of analysis generally requires invasive measurement of continuous LV pressure and is usually reserved for the cardiac catheterization laboratory. Several indices of LV relaxation may be derived using this method, among which the maximum rate of LV pressure decline ( $-\text{dP}/\text{dt}$ ; analogous to  $+\text{dP}/\text{dt}$  during isovolumic contraction) and a time constant ( $\tau$ ) of LV relaxation are the most common. LV  $-\text{dP}/\text{dt}$  is not an ideal as an index of LV relaxation because this parameter is essentially a “snapshot” of relaxation that is affected by the value of LV endsystolic pressure. LV pressure decay during relaxation is exponential between aortic valve closure and mitral valve opening. A time constant ( $\tau$ ) derived using the equation:  $P(t) = P_0 e^{-t/\tau}$ , where  $P(t)$  is time-dependent LV pressure,  $P_0$  is LV pressure at end-systole,  $e$  is the natural exponent, and  $t$  is time after LV end-systole, is used to quantify relaxation. Despite the limitations of this simple model,<sup>85, 86</sup> an increase in  $\tau$  indicates that a delay in LV relaxation has occurred. This technique has been used to quantify delays in LV relaxation during cardiac disease (e.g., myocardial ischemia,<sup>87</sup> pressure-overload hypertrophy<sup>88</sup>) or as a result of administration of negative inotropic medications including volatile anesthetics.<sup>89</sup> In contrast, reductions in  $\tau$  (indicative of more rapid relaxation) are observed during tachycardia, sympathetic nervous system activation, or administration of positive inotropic drugs. From a clinical standpoint, LV relaxation and its pharmacologic modulation are very important in heart failure. LV relaxation is modestly dependent on afterload under normal conditions,<sup>27</sup> but this afterload-sensitivity of LV relaxation is especially pronounced in the failing heart.<sup>90</sup> Thus, medications that reduce afterload not only augment LV systolic function but also simultaneously enhance LV relaxation (decrease  $\tau$ ) in patients with heart failure.<sup>68</sup> This latter effect improves early LV filling dynamics and reduces congestive signs and symptoms.

### ***Invasive Assessment of LV Filling and Compliance***

**13** Indices of LV filling may be calculated using invasive or noninvasive (e.g., two- or three-dimensional echocardiography, radionuclide angiography, cardiac MRI) measurement of continuous LV volume. The first derivative of LV volume waveform with respect to time ( $\text{dV}/\text{dt}$ ) creates a biphasic waveform with peaks occurring during early LV filling (E) and atrial systole (A). The transmitral blood flow velocity signal acquired during LV filling using pulse wave Doppler echocardiography (see below) closely resembles this  $\text{dV}/\text{dt}$  waveform. Development of heart failure causes characteristic changes in  $\text{dV}/\text{dt}$  morphology that are identical to the “delayed relaxation,” “pseudonormal,” and “restrictive” filling patterns measured using pulse wave Doppler (Fig. 12-19).<sup>91</sup> Invasive analysis of LV filling with continuous LV volume and its first derivative is limited almost exclusively to the laboratory and is of little practical value in clinical anesthesiology except as a teaching tool.

As mentioned earlier in the discussion, EDPVR is an index of LV compliance derived from a nested set of LV P-V diagrams. The relationship between end-diastolic pressure (EDP) and EDV is exponential such that  $\text{EDP} =$

$Ae^{K(EDV)} + B$ , where  $K$  is the modulus of chamber stiffness and  $A$  and  $B$  are curve-fitting constants. An increase in  $K$  indicates that the LV is less compliant, that is, higher LV pressure is required to distend the LV to a given volume. Parallel upward shifts in the EDPVR, such as seen in pericardial tamponade, represent an exception, because the value of  $K$  remains constant under these circumstances even though LV pressure is greater at each LV volume.<sup>52</sup> Thus, the relative position of the EDPVR in P-V phase space may be more important than the actual value of  $K$  itself because a shift in EDPVR up or to the left indicates that a higher LV pressure is required to achieve a similar LV volume.<sup>92</sup>

The diastolic stress-strain relation is another model frequently used to experimentally describe LV compliance. Myocardium is

P.295

an elastic material that follows Hooke law, developing resisting forces (stress;  $\sigma$ ) as muscle length (strain;  $\epsilon$ ) increases during LV filling. The relationship is also exponential such that  $\sigma = \alpha(e^{\beta\epsilon} - 1)$ , where  $\alpha$  is the coefficient of gain and  $\beta$  is the modulus of myocardial stiffness.<sup>93</sup> Similar to the EDPVR, an increase in  $\beta$  occurs when the stress-strain relationship shifts up or to the left and may be observed in pathologic conditions characterized by fundamental structural abnormalities that adversely influence myocardial stiffness (e.g., hypertrophic cardiomyopathy, amyloidosis). EDPVR and myocardial stress-strain relations are generally not used clinically because analysis required to examine these relationships is complicated, time-consuming, and limited to steady-state hemodynamic conditions.

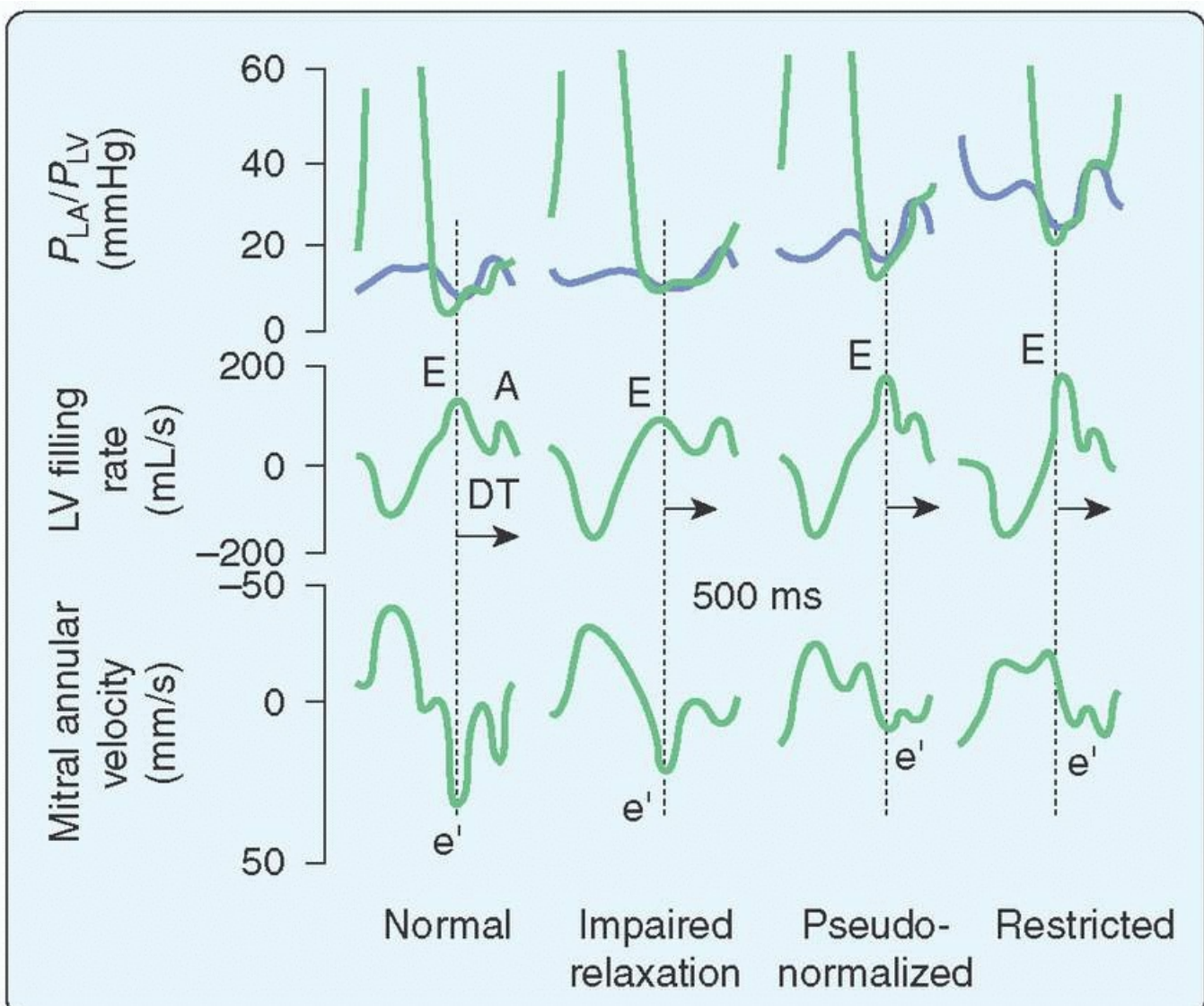


**Figure 12-19** This illustration depicts the simultaneous relationships between LA and LV pressures ( $P_{LA}$  and  $P_{LV}$ , respectively; top panels), LV filling rate during early filling (E) and atrial systole (A; middle panels), and early mitral annular velocity (e; bottom panels) under normal conditions and during evolving diastolic dysfunction (impaired relaxation, pseudonormal, and restrictive). Note the initial lengthening of E wave deceleration time (DT) during impaired relaxation and the subsequent shortening of DT as diastolic function worsens. (Reproduced with permission from Kaplan JA, Reich DL, Savino JS. *Kaplan's Cardiac Anesthesia: The Echo Era*. 6th ed. St. Louis, MO: Elsevier Saunders; 2011:122.)

### **Noninvasive Evaluation of Diastolic Function**

The duration between aortic valve closure (end-systole) and mitral valve opening (onset of transmitral blood flow) defines isovolumic relaxation time (IVRT), a commonly used noninvasive index of LV relaxation that is usually measured using M-mode or pulse wave Doppler echocardiography. The rate of LV relaxation and the difference between LV end-systolic pressure and LA pressure when the mitral valve opens determines IVRT in the absence of aortic or mitral valve disease.<sup>94</sup> It should be readily apparent that IVRT is dependent on both LV relaxation and loading conditions. Indeed, IVRT is seldom used alone to quantify LV relaxation, but is most often combined with the transmitral blood flow velocity pattern to more comprehensively define the rate and extent of LV relaxation.

Noninvasive analysis of LV diastolic function is based on Doppler echocardiographic evaluation of transmitral blood flow velocity.<sup>95</sup> A pulse wave Doppler echocardiography sample volume is placed between the tips of the mitral leaflets to obtain a high-resolution transmitral blood flow velocity envelope. The normal pattern of transmitral blood flow velocity has two peaks: an early “E” peak associated with early LV filling and a late “A” peak corresponding to LA systole.<sup>96</sup> The ratio of the peak E and A wave velocities is commonly used to quantify the relative contributions of early LV filling and atrial systole to EDV. The time elapsed as the E wave velocity declines from its peak value to zero is known as the deceleration time; this parameter is often used with IVRT to quantify LV relaxation. For example, an increase in E wave deceleration time indicates that early LV filling is prolonged because LV relaxation is delayed. Age affects LV diastolic function because a progressive slowing of LV relaxation occurs. As a result, IVRT, deceleration time, and A wave velocity increase with age, whereas E wave velocity and E/A ratio decrease.<sup>97</sup> The aging heart becomes less compliant, especially in the presence of coexisting essential hypertension and LV hypertrophy. This change predisposes the elderly to develop heart failure.<sup>98</sup>

The reversal of E/A with advancing age is an example of a “delayed relaxation” pattern of LV diastolic dysfunction. This transmitral blood flow velocity pattern is the least severe of three abnormal LV filling patterns that describe the continuum of abnormal LV diastolic function. Clinical symptoms, exercise tolerance, New York Heart Association (NYHA) functional class, and mortality are closely correlated with the relative severity of LV diastolic dysfunction quantified using this method.<sup>99</sup> E/A <1 characterizes “delayed relaxation” and indicates that early LV filling is attenuated and the LA's contribution to filling is enhanced (atrial kick).<sup>91</sup> The “delayed relaxation” pattern is often observed in patients with essential hypertension, pressure-overload LV hypertrophy, and myocardial ischemia (Fig. 12-20).

As diastolic dysfunction worsens, a “pseudonormal” pattern replaces the “delayed relaxation” profile. This pseudonormal pattern occurs because E/A becomes >1 (similar to the normal profile, thus the term “pseudonormal”) as LA pressures increase to compensate for the further reduction in LV compliance. Thus, E wave velocity “normalizes” because the LA-LV pressure gradient increases when the mitral valve opens. Other indices of diastolic function (e.g., pulmonary venous blood flow velocity, tissue Doppler imaging) are required to

distinguish the “pseudonormal” from a normal transmitral blood flow velocity profile. Alternatively, administration of a small bolus of a vasodilator (e.g., nitroglycerin) may convert a “pseudonormal” profile into a “delayed relaxation” pattern by transiently reducing LA pressure.<sup>100</sup> A “restrictive pattern” of transmitral blood flow velocity is the most severe form of LV diastolic dysfunction in which LA hypertension is present and LV compliance is further reduced. The E/A becomes >2 as the LA-LV pressure gradient is further augmented by increased LA pressure (causing a larger peak E wave velocity), concomitant with progressive LA contractile dysfunction (decline in peak A wave velocity). Failure of a “restrictive” filling pattern to respond to administration of a vasodilator and revert to a “pseudonormal” or “delayed relaxation” pattern carries a grim prognosis in patients with heart failure, unless a mechanical circulatory support device is implanted or cardiac transplantation is performed.<sup>95</sup>

**14** Abnormal LV diastolic function may also be determined using analysis of the pulmonary venous blood flow velocity pattern obtained with pulse wave Doppler echocardiography.<sup>101</sup> Most often, the pulmonary venous blood flow velocity is used in combination with transmitral blood flow velocity when quantifying the severity of LV diastolic dysfunction.<sup>102</sup> Two large positive deflections (forward flow from the pulmonary veins into the LA) and a single, small negative deflection

P.296

(retrograde flow from the LA to the pulmonary veins, termed “atrial reversal”) establish the normal pulmonary venous blood flow velocity pattern. The first positive deflection is known as the “S” (systolic) wave, and occurs while the mitral valve is closed (LV systole and early diastole).<sup>103</sup> This “S” wave results from LA relaxation, which stimulates forward movement of blood from the pulmonary veins into the LA. The mitral valve annulus also descends toward the LV apex during systole, drawing additional blood from the pulmonary veins into the LA (similar to an engine piston).<sup>104</sup> This latter action is attenuated when LV contractility is depressed, emphasizing that the LV systolic function has a direct impact on LA filling. Transmission of the RV systolic pressure pulse through the pulmonary circulation further contributes to LA filling. After the mitral valve opens, blood stored in the LA during LV systole enters the LV, an event which allows additional blood to flow from the pulmonary veins into the LA. This causes the second positive deflection (“D” [diastolic] wave) of the pulmonary venous blood flow velocity pattern. The “D” wave is dependent on the extent of early LV filling and LV compliance.<sup>105</sup> LA preload, LA contractility, and LV pressure during late diastole determine the magnitude of the “atrial reversal” (Ar) wave.<sup>106</sup>

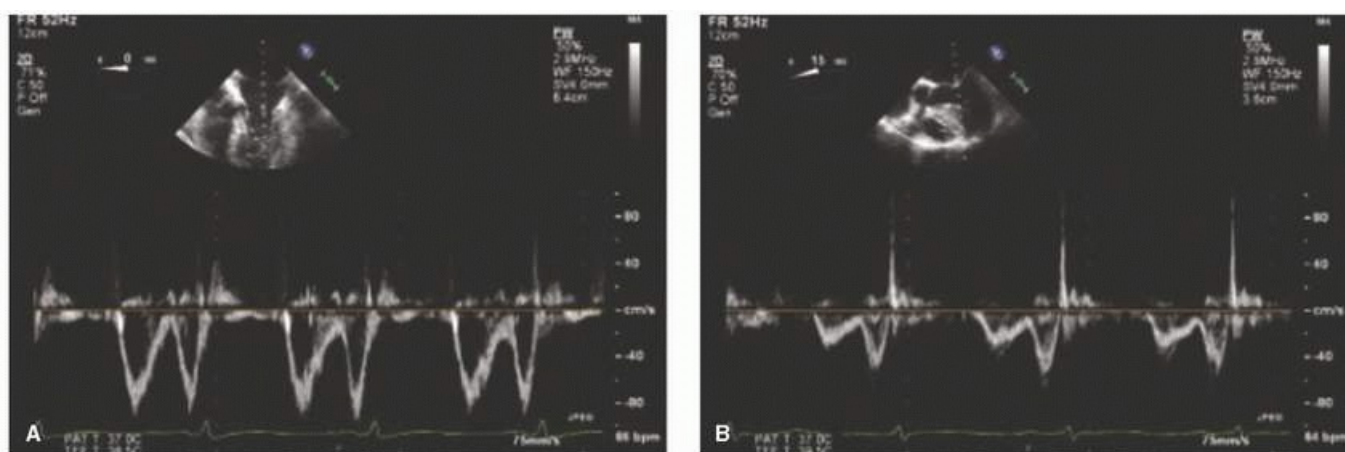


**Figure 12-20** Transmitral blood flow velocity waveforms obtained using pulse wave Doppler echocardiography under normal conditions (left) and during delayed relaxation (right). (Reproduced with permission from Kaplan JA, Reich DL, Savino JS. *Kaplan's Cardiac Anesthesia: The Echo Era*. 6th ed. St. Louis, MO: Elsevier

The ratio of “S” to “D” waves and the peak velocity of the “Ar” wave increase with age.<sup>96</sup> These findings emphasize that LA function is more important to LV filling in the elderly. As LV diastolic function worsens, LA pressures increase and the “S” wave is attenuated (Fig. 12-21). The presence of this blunted “S” wave allows the echocardiographer to distinguish between normal and “pseudonormal” transmitral blood flow velocity patterns because  $S/D < 1$  in the latter condition.<sup>101</sup> Such alterations in S/D become even more exaggerated in the presence of a “restrictive” filling pattern because LV diastolic and LA pressures are further elevated. Indeed, the “S” wave may be entirely abolished or even reversed (blood flow refluxing from the LA into the pulmonary veins) concomitant with an enhanced “D” wave in the presence of “restrictive” pathophysiology. Thus, pulmonary venous blood flow velocity patterns provide very useful information about LV diastolic dysfunction. Pulmonary venous blood flow patterns are also important when grading the severity of mitral regurgitation because LA pressure rises rapidly during the “S” phase as a result of regurgitant blood flow from the LV to the LA. Profound blunting or reversal of the “S” wave under these circumstances indicates that moderate or severe mitral regurgitation is present, respectively. Other indices of diastolic function, including tissue Doppler imaging<sup>107</sup> and color M-mode propagation velocity,<sup>108</sup> may also be used to define the progression of LV diastolic dysfunction. The reader is referred to Chapter 27 for a detailed discussion of the echocardiographic assessment of diastolic function.

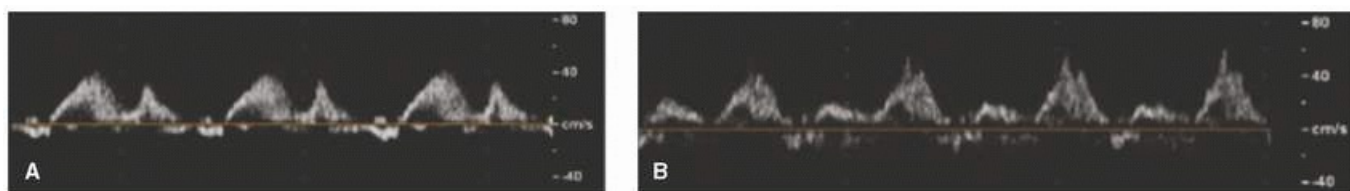


**Figure 12-21** Pulmonary venous blood flow velocity waveforms obtained using pulse wave Doppler echocardiography under normal conditions (left panel) and in the presence of increased LA pressure (right panel). (Reproduced with permission from Kaplan JA, Reich DL, Savino JS. *Kaplan's Cardiac Anesthesia: The Echo Era*. 6th ed. St. Louis, MO: Elsevier Saunders; 2011:125.)

## Pericardium

**15 16** The pericardium contains the heart, proximal great vessels, vena cavae, and pulmonary veins. The pericardium acts to separate the heart from other structures in the mediastinum and limits the heart's movement through its diaphragmatic and great vessel attachments. The fluid in the pericardium acts as a lubricant and consists of a combination of plasma ultrafiltrate, lymph, and myocardial interstitial fluid (total volume of 15 to 35 mL). The pericardium is much less compliant than myocardium, and has very limited volume reserve (Fig. 12-22).<sup>109</sup> As a result, an acute increase in pericardial volume (e.g., tamponade) causes a

P.297

pronounced elevation in pericardial pressure that substantially restricts filling of the cardiac chambers.<sup>110</sup> The pericardium normally restrains expansion of the low-pressure atria and RV because these chambers have thinner walls than the LV. Indeed, pericardial restraint is the primary determinant of the diastolic pressure-volume relations of the RA, LA, and RV, whereas the compliance of these chambers alone is less important. The pericardium also profoundly affects LV filling.<sup>111</sup> As mentioned earlier, a parallel upward shift of the EDPVR occurs in response to an acute increase in pericardial pressure.<sup>112</sup> This shift in the EDPVR indicates that LV pressure must be greater for each LV volume and explains why LV filling is impaired during tamponade physiology. While the pericardium is acutely noncompliant, a slow increase in pericardial pressure (e.g., chronic



pericardial effusion or biventricular dilatation) causes the pericardium to gradually expand in size. This compensatory response increases the pericardium's compliance and reduces its restraining forces, thereby allowing the heart to continue functioning without imminent hemodynamic collapse.

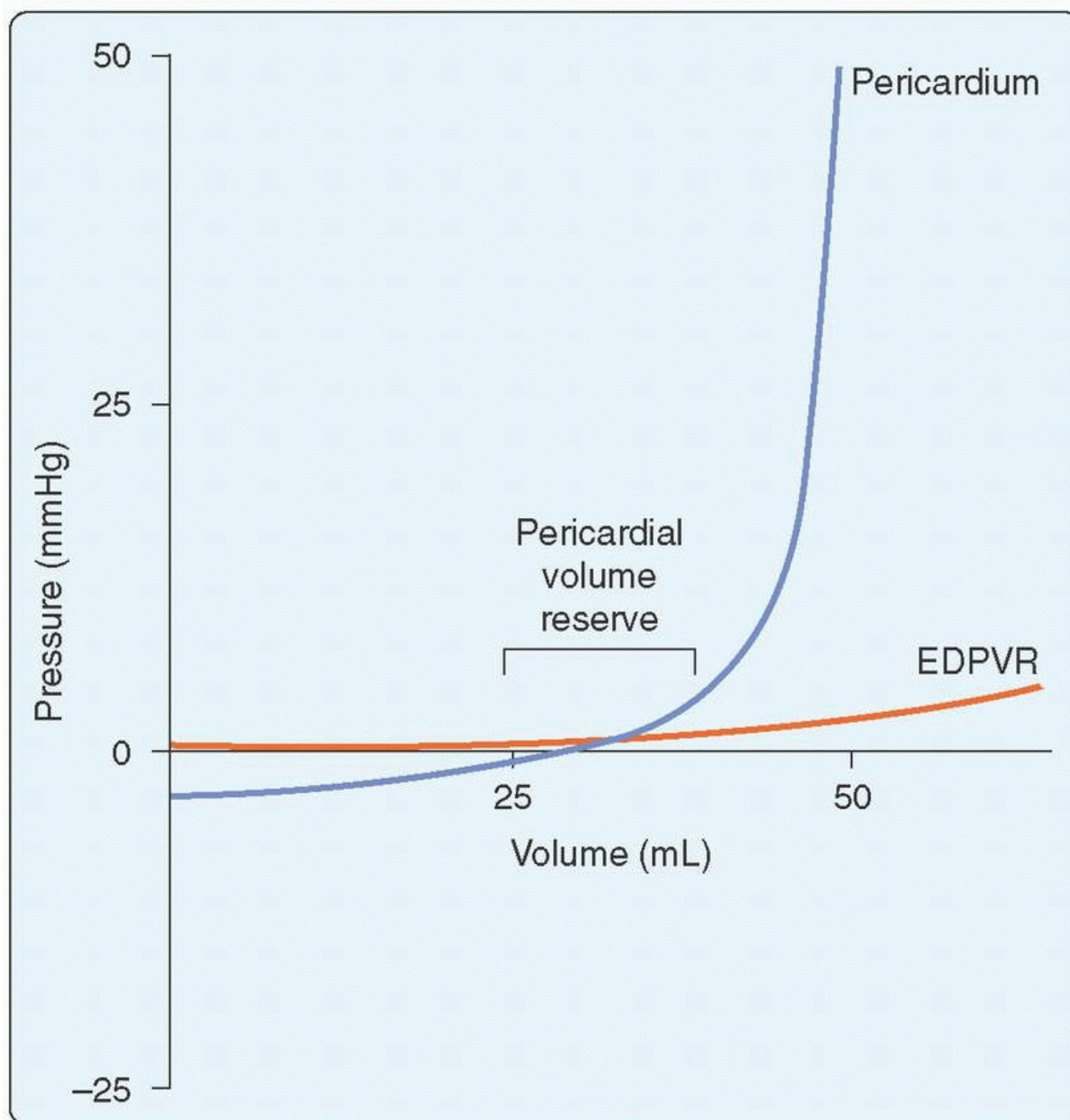


**Figure 12-22** Pressure-volume relation of the pericardium (*blue line*) compared with the LV end-diastolic pressure-volume relation (EDPVR; *red line*). Note that large increases in pericardial volume occur after reserve volume is exceeded. (Reproduced with permission from Kaplan JA, Reich DL, Savino JS. *Kaplan's Cardiac Anesthesia: The Echo Era*. 6th ed. St. Louis, MO: Elsevier Saunders; 2011:127.)

Ventricular interdependence is the influence of the pressure and volume of one ventricle on the function of the other. The pericardium plays a central role in ventricular interdependence because it provides equal restraint of the RV and the LV. As a result, a rapid increase in RV pressure and volume (e.g., volume overload, acute increase in pulmonary arterial pressure) causes the pressure within the pericardium to increase as well. This action compresses the LV, reducing its effective compliance and impairing its filling.<sup>113</sup> Not surprisingly, LV distention has a similar effect on the RV and limits RV filling through an identical mechanism.<sup>114</sup> Ventricular interdependence may be readily appreciated by examining changes in RV and LV filling during spontaneous

ventilation.<sup>115</sup> Because intrathoracic pressure declines during inspiration, venous return to the right side of the heart increases and produces modest dilation of the RV. The result of this RV distention is a corresponding increase in pericardial restraint of the LV, which limits LV filling and causes a small decrease in stroke volume and mean arterial pressure. This ventricular interaction effect between the RV and LV is reversed during expiration. Directly opposite effects on RV and LV filling occur during inspiration and expiration in the presence of positive-pressure ventilation. The hemodynamic consequences of ventricular interdependence form the basis of respiratory cycle-induced pulse pressure and stroke volume variation, which have been shown to be useful dynamic indices of preload in conscious and anesthetized patients.<sup>116</sup> Notably, pericardial tamponade<sup>117</sup> or constrictive pericarditis<sup>118</sup> exaggerates the normal respiratory changes in RV and LV filling and produces pulsus paradoxus. It is especially important to appreciate that spontaneous ventilation is crucial in these conditions because negative intrathoracic pressure assists venous return, whereas cardiovascular collapse may occur with the initiation of positive pressure ventilation because venous return becomes profoundly limited.

### ***Atrial Function***

The mechanical properties of the LA are often overlooked in discussions of cardiac physiology. This is unfortunate because the LA acts as a contractile chamber, a reservoir (storage of blood before mitral valve opening), and a conduit (an extension of the pulmonary veins). The LA's function is critical to LV performance. The maximum velocity of shortening of LA myocardium is equal to or greater than LV myocardium under similar loading conditions.<sup>119</sup> LA emptying fraction (similar to LV EF) is dependent on LA contractility, preload, and LV compliance, unless the LA becomes so dilated that its myofilaments are stretched far beyond their normal operating length.<sup>120</sup> This magnitude of LA dilation may occur when LA pressures are chronically elevated because of severe LV diastolic dysfunction or mitral regurgitation. Under these conditions, the LA may no longer be capable of contributing to EDV as a contractile chamber. The LA's response to changes in autonomic nervous system activity, inotropic medications, and anesthetics is very similar to that of the LV.<sup>121, 122</sup> LV compliance and pressure during late diastole determine the afterload with which the LA is confronted during its contraction. Thus, the LA must perform greater work in the presence of LV diastolic dysfunction because its afterload is increased. Like the RV, the LA is more susceptible to acute increases in afterload than is the LV, because the LA has less muscle mass and thinner walls. As a result, the LA emptying fraction may initially increase early during developing LV failure,<sup>123</sup> but subsequently decline as LA contractile dysfunction occurs concomitant with chamber dilatation.<sup>124</sup> LV diastolic dysfunction also causes remodeling and reduced compliance of the LA, which also further limit pulmonary venous return.

The LA also serves reservoir and conduit functions. LA relaxation, LV base descent during systole, transmission of RV stroke volume, and LA compliance determine LA reservoir function. LA ischemia, hypertrophy, or dilation attenuate reservoir function, as do LV or RV contractile dysfunction.<sup>104, 106</sup> Disease states in which LA compliance is selectively reduced are associated with impaired LA filling and contribute to pulmonary venous congestion.<sup>46, 125</sup> The LA appendage plays an important role in LA filling, as exclusion or excision of the LA appendage reduces the compliance of the LA chamber as a whole.<sup>126, 127</sup> LA appendage exclusion procedures are often performed during cryoablation

P.298

for treatment of chronic atrial fibrillation, and reduced LA compliance concomitant with elevated pulmonary venous pressures may be anticipated despite restoration of sinus rhythm.

Exercise enhances both LA contractility and reservoir function.<sup>128</sup> The latter effect is important because greater reservoir capacity causes a larger LA-LV pressure gradient during early LV filling, thereby facilitating additional

blood flow to the LV during conditions requiring greater LV stroke volume and cardiac output. Conduit function is also augmented in endurance athletes.<sup>129</sup> As the LA begins to dilate in healthy elderly subjects, compensatory increases in LA emptying fraction and declines in passive LA emptying occur.<sup>130</sup> LA dilation initially augments the ratio of LA reservoir to LV stroke volume (termed “storage fraction”),<sup>131</sup> but this beneficial effect comes at a cost: the dilation increases in LA wall stress, which may contribute to eventual LA contractile dysfunction and the development of atrial arrhythmias.<sup>132</sup>

## REFERENCES

1. Buckberg GD, Coghlan HC, Torrent-Guasp F. The structure and function of the helical heart and its buttress wrapping. VI. Geometric concepts of heart failure and use for structural correction. *Semin Thorac Cardiovasc Surg.* 2001;13:386-401.
2. Cheng C-P, Noda T, Nozawa T, et al. Effect of heart failure on the mechanism of exercise-induced augmentation of mitral valve flow. *Circ Res.* 1993;72:795-806.
3. Takayama Y, Costa KD, Covell JW. Contribution of laminar myofiber architecture to load-dependent changes in mechanics of LV myocardium. *Am J Physiol Heart Circ Physiol.* 2002;282:H1510-H1520.
4. Gharib M, Rambod E, Kheradvar A, et al. Optimal vortex formation as an index of cardiac health. *Proc Natl Acad Sci U S A.* 2006;103:6305-6308.
5. Sidebotham DA, Allen SJ, Gerber IL, et al. Intraoperative transesophageal echocardiography for surgical repair of mitral regurgitation. *J Am Soc Echocardiogr.* 2014;27:345-366.
6. Pagel PS, Diciaula G, Schroeder AR. Edible model of mitral valve leaflet surface geometry. *J Cardiothorac Vasc Anesth.* 2015;29:e4-e5.
7. Montealegre-Gallegos M, Bergman R, Jiang L, et al. Tricuspid valve: an intraoperative echocardiographic perspective. *J Cardiothorac Vasc Anesth.* 2014;28:761-770.
8. Voci P, Bilotta F, Caretta Q, et al. Papillary muscle perfusion pattern. A hypothesis for ischemic papillary muscle dysfunction. *Circulation.* 1995;91:1714-1718.
9. Stefanadis C, Dernellis J, Tsiamis E, et al. Effects of pacing-induced and balloon coronary occlusion ischemia on left atrial function in patients with coronary artery disease. *J Am Coll Cardiol.* 1999;33:687-696.
10. Katti K, Patil NP. The Thebesian valve: gatekeeper to the coronary sinus. *Clin Anat.* 2012;25:379-385.
11. Tops LF, Schalij MJ, Bax JJ. The effects of right ventricular apical pacing on ventricular function and dyssynchrony implications for therapy. *J Am Coll Cardiol.* 2009;54:764-776.
12. Epstein AE, DiMarco JP, Ellenbogen KA, et al. ACC/AHA/HRS 2008 Guidelines for Device-Based Therapy of Cardiac Rhythm Abnormalities: a report of the American College of Cardiology/American Heart Association Task Force on Practice Guidelines (Writing Committee to Revise the ACC/AHA/NASPE 2002

Guideline Update for Implantation of Cardiac Pacemakers and Antiarrhythmia Devices): developed in collaboration with the American Association for Thoracic Surgery and Society of Thoracic Surgeons. *Circulation*. 2008;117:e350-e408.

---

13. Gorman MW, Tune JD, Richmond KN, et al. Feedforward sympathetic coronary vasodilation in exercising dogs. *J Appl Physiol*. 2000;89:1892-1902.

---

14. Gorman MW, Rooke GA, Savage MV, et al. Adenine nucleotide control of coronary blood flow during exercise. *Am J Physiol Heart Circ Physiol*. 2010;299:H1981-H1989.

---

15. Schaub MC, Hefti MA, Zuellig RA, et al. Modulation of contractility in human cardiac hypertrophy by myosin essential light chain isoforms. *Cardiovasc Res*. 1998;37:381-404.

---

16. Cazorla O, Vassort G, Garnier D, et al. Length modulation of active force in rat cardiac myocytes: is titin the sensor? *J Mol Cell Cardiol*. 1999;31:1215-1227.

---

17. Helmes M, Trombitas K, Granzier H. Titin develops restoring force in rat cardiac myocytes. *Circ Res*. 1996;79:619-626.

---

18. Schiaffino S, Reggiani C. Molecular diversity of myofibrillar proteins: gene regulation and molecular significance. *Physiol Rev*. 1996;76:371-423.

---

19. Moncman CL, Wang K. Nebulette: a 107 kD nebulin-like protein in cardiac muscle. *Cell Motil Cytoskel*. 1995;32:205-225.

---

20. Solaro RJ, Rarick HM. Troponin and tropomyosin. Proteins that switch on and tune in the activity of cardiac myofilaments. *Circ Res*. 1998;83:471-480.

---

21. Tobacman LS. Thin filament-mediated regulation of cardiac contraction. *Annu Rev Physiol*. 1996;58:447-481.

---

22. Solaro RJ, Van Eyk J. Altered interactions among thin filaments proteins modulate cardiac function. *J Mol Cell Cardiol*. 1999;28:217-230.

---

23. Luo W, Grupp IL, Harrer J, et al. Targeted ablation of the phospholamban gene is associated with markedly enhanced myocardial contractility and loss of  $\beta$ -agonist stimulation. *Circ Res*. 1994;75:401-409.

---

24. Rayment I, Holden HM, Whittaker M. Structure of the actin-myosin complex and its implications for muscle contraction. *Science*. 1993;261:58-65.

---

25. Dominguez R, Freyzo Y, Trybus KM, et al. Crystal structure of a vertebrate smooth muscle myosin motor domain and its complex with the essential light chain: visualization of the prepower stroke state. *Cell*. 1998;94:559-571.

---

26. Finer JT, Simmons RM, Spudich JA. Single myosin molecule mechanics: piconewton forces and

nanometer steps. *Nature*. 1994;368:113-119.

---

27. Gilbert JC, Glantz SA. Determinants of left ventricular filling and of the diastolic pressure-volume relation. *Circ Res*. 1989;64:827-852.

---

28. Grossman W, Jones D, McLaurin LP. Wall stress and patterns of hypertrophy in the human left ventricle. *J Clin Invest*. 1975;56:56-64.

---

29. Florenzano F, Glantz SA. Left-ventricular mechanical adaptation to chronic aortic regurgitation in intact dogs. *Am J Physiol*. 1987;252:H969-H984.

---

30. Regen DM. Calculation of left ventricular wall stress. *Circ Res*. 1990;67: 245-252.

---

31. Regen DM, Anversa P, Capasso JM. Segmental calculation of left ventricular wall stresses. *Am J Physiol*. 1993;264:H1411-H1421.

---

32. Wiggers CJ. The Henry Jackson Memorial Lecture. Dynamics of ventricular contraction under abnormal conditions. *Circulation*. 1952;5:321-348.

---

33. Haddad F, Couture P, Tousignant C, et al. The right ventricle in cardiac surgery, a perioperative perspective: I. Anatomy, physiology, and assessment. *Anesth Analg*. 2009;108:407-421.

---

34. Haddad F, Couture P, Tousignant C, et al. The right ventricle in cardiac surgery, a perioperative perspective: II. Pathophysiology, clinical importance, and management. *Anesth Analg*. 2009;108:422-433.

---

35. Cheng C-P, Freeman GL, Santamore WP, et al. Effect of loading conditions, contractile state, and heart rate on early diastolic left ventricular filling in conscious dogs. *Circ Res*. 1990;66:814-823.

---

36. Courtois M, Kovacs SJ Jr, Ludbrook PA. Transmitral pressure-flow velocity relation. Importance of regional pressure gradients in the left ventricle during diastole. *Circulation*. 1988;78:661-671.

---

37. Ishida Y, Meisner JS, Tsujioka K, et al. Left ventricular filling dynamics: influence of left ventricular relaxation and left atrial pressure. *Circulation*. 1986;74:187-196.

---

38. Little WC, Oh JK. Echocardiographic evaluation of diastolic function can be used to guide clinical care. *Circulation*. 2009;120:802-809.

---

39. Kheradvar A, Gharib M. On mitral valve dynamics and its connection to early diastolic flow. *Ann Biomed Eng*. 2009;37:1-13.

---

40. Pagel PS, Gandhi SD, Iqbal Z, et al. Cardiopulmonary bypass transiently inhibits intraventricular vortex ring formation in patients undergoing coronary artery bypass graft surgery. *J Cardiothorac Vasc Anesth*. 2012;26:376-380.

---

41. Pagel PS, Hudetz JA. Chronic pressure-overload hypertrophy attenuates vortex formation time in patients

with severe aortic stenosis and preserved left ventricular systolic function undergoing aortic valve replacement. *J Cardiothorac Vasc Anesth.* 2013;27:660-664.

---

42. Yellin EL, Nikolic S, Frater RWM. Left ventricular filling dynamics and diastolic function. *Prog Cardiovasc Dis.* 1990;32:247-271.

---

43. Suga H, Yasumura Y, Nozawa T, et al. Pressure-volume relation around zero transmural pressure in excised cross-circulated dog left ventricle. *Circ Res.* 1988;63:361-372.

---

44. Keren G, Meisner JS, Sherez J, et al. Interrelationship of mid-diastolic mitral valve motion, pulmonary venous flow, and transmitral flow. *Circulation.* 1986; 74:36-44.

---

45. Barbier P, Solomon SB, Schiller NB, et al. Left atrial relaxation and left ventricular systolic function determine left atrial reservoir function. *Circulation.* 1999;100:427-436.

---

46. Mehta S, Charbonneau F, Fitchett DH, et al. The clinical consequences of a stiff left atrium. *Am Heart J.* 1991;122:1184-1191.

---

47. Sagawa K. The end-systolic pressure-volume relation of the ventricle: definition, modifications and clinical use. *Circulation.* 1981;63:1223-1227.

---

48. Kass DA, Maughan WL, Guo ZM, et al. Comparative influence of load versus inotropic states on indexes of ventricular contractility: experimental and theoretical analysis based on pressure-volume relationships. *Circulation.* 1987;76: 1422-1436.

---

49. Suga H. Ventricular energetics. *Physiol Rev.* 1990;70:247-277.

---

50. Brown KA, Ditchey RV. Human right ventricular end-systolic pressure-volume relation defined by maximal elastance. *Circulation.* 1988;78:81-91.

---

51. Pagel PS, Kehl F, Gare M, et al. Mechanical function of the left atrium: new insights based on analysis of pressure-volume relations and Doppler echocardiography. *Anesthesiology.* 2003;98:975-994.

---

52. Grossman W. Diastolic dysfunction and congestive heart failure. *Circulation.* 1990;81(2 suppl):III1-7.

---

53. Little WC, Downes TR. Clinical evaluation of left ventricular diastolic performance. *Prog Cardiovasc Dis.* 1990;32:273-290.

---

P.299

54. Wier W, Yue DT. Intracellular  $[Ca^{++}]$  transients underlying the short-term force-interval relationship in ferret ventricular myocardium. *J Physiol (Lond).* 1986;376:507-530.

---

55. Vatner SF. Sympathetic mechanisms regulating myocardial contractility in conscious animals. In: Fozzard HA, Haber E, Jennings RB, et al., eds. *The Heart and Cardiovascular System: Scientific Foundations.* 2nd ed. New York: Raven Press; 1991:1709-1728.

- 
56. Little WC, Freeman GL, O'Rourke RA. Simultaneous determination of left ventricular end-systolic pressure-volume and pressure-dimension relationships in closed-chest dogs. *Circulation*. 1985;71:1301-1308.
- 
57. Burkhoff D. The conductance method of left ventricular volume estimation. Methodologic limitations put into perspective. *Circulation*. 1990;81:703-706.
- 
58. Dorosz JL, Lezotte DC, Weitzenkamp DA, et al. Performance of 3-dimensional echocardiography in measuring left ventricular volumes and ejection fraction: a systematic review and meta-analysis. *J Am Coll Cardiol*. 2012;59:1799-1808.
- 
59. Cowie B, Kluger R, Kalpokas M. Left ventricular volume and ejection fraction assessment with transoesophageal echocardiography: 2D vs 3D imaging. *Br J Anesth*. 2013;110:201-206.
- 
60. Meris A, Santambrogio L, Casso G, et al. Intraoperative three-dimensional versus two-dimensional echocardiography for left ventricular assessment. *Anesth Analg*. 2014;118:711-720.
- 
61. Hansen RM, Viquerat CE, Matthay MA, et al. Poor correlation between pulmonary arterial wedge pressure and left ventricular end-diastolic volume after coronary artery bypass graft surgery. *Anesthesiology*. 1986;64:764-770.
- 
62. Tousignant C, Van Orman JR. Pulmonary impedance and pulmonary Doppler trace in the perioperative period. *Anesth Analg*. 2015;121:601-609.
- 
63. Borow KM, Colan SD, Neumann A. Altered left ventricular mechanics in patients with valvular aortic stenosis and coarctation of the aorta: effects on systolic performance and late outcome. *Circulation*. 1985;72:515-522.
- 
64. Weber KT, Janicki JS. Myocardial oxygen consumption: the role of wall force and shortening. *Am J Physiol*. 1977;233:H421-H430.
- 
65. Little WC, Cheng CP. Left ventricular-arterial coupling in conscious dogs. *Am J Physiol*. 1991;261:H70-H76.
- 
66. Nichols WW, Nicolini FA, Pepine CJ. Determinants of isolated systolic hypertension in the elderly. *J Hypertens*. 1992;10:S73-S77.
- 
67. Lang RM, Borow KM, Neumann A, et al. Systemic vascular resistance: an unreliable index of left ventricular afterload. *Circulation*. 1986;74:1114-1123.
- 
68. Little WC. Enhanced load dependence of relaxation in heart failure. Clinical implications. *Circulation*. 1992;85:2326-2328.
- 
69. de Tombe PP, Little WC. Inotropic effects of ejection are myocardial properties. *Am J Physiol*.

1994;266:H1202-H1213.

---

70. Suga H, Sagawa K, Shoukas AA. Load-independence of the instantaneous pressure-volume ratio of the canine left ventricle and effects of epinephrine and heart rate on the ratio. *Circ Res*. 1973;32:314-322.

---

71. Glower DD, Spratt JA, Snow ND, et al. Linearity of the Frank-Starling relationship in the intact heart: the concept of preload recruitable stroke work. *Circulation*. 1985;71:994-1009.

---

72. Chen C, Rodriguez L, Guerrero JL, et al. Noninvasive estimation of the instantaneous first derivative of left ventricular pressure using continuous-wave Doppler echocardiography. *Circulation*. 1991;83:2101-2110.

---

73. Little WC. The left ventricular dP/dtmax-end-diastolic volume relation in closed-chest dogs. *Circ Res*. 1985;56:808-815.

---

74. Yew WYW. Evaluation of left ventricular diastolic function. *Circulation*. 1989;79:1393-1397.

---

75. Gaasch WH, Zile MR. Left ventricular diastolic dysfunction and diastolic heart failure. *Annu Rev Med*. 2004;55:373-394.

---

76. Maeder MT, Kaye DM. Heart failure with normal left ventricular ejection fraction. *J Am Coll Cardiol*. 2009;53:905-918.

---

77. Zile MR, Baicu CF, Gaasch WH. Diastolic heart failure - abnormalities in active relaxation and passive stiffness of the left ventricle. *N Engl J Med*. 2004;350:1953-1959.

---

78. Bench T, Burkhoff D, O'Connell JB, et al. Heart failure with normal ejection fraction: consideration of mechanisms other than diastolic dysfunction. *Curr Heart Fail Rep*. 2009;6:57-64.

---

79. Grewal J, McCully RB, Kane GC, et al. Left ventricular function and exercise capacity. *JAMA*. 2009;301:286-294.

---

80. Traversi E, Pozzoli M, Cioffi G, et al. Mitral flow velocity changes after 6 months of optimized therapy provides important hemodynamic and prognostic information in patients with heart failure. *Am Heart J*. 1996;132:809-819.

---

81. Pagel PS, Farber NE. Inhaled anesthetics: cardiovascular pharmacology. In: Miller R D, Cohen N, Eriksson LI, et al. *Miller's Anesthesia*, 8th ed. Philadelphia, PA: Elsevier Churchill Livingstone; 2014:706-751.

---

82. Flu WJ, van Kuijk JP, Hoeks SE, et al. Prognostic implications of asymptomatic left ventricular dysfunction in patients undergoing vascular surgery. *Anesthesiology*. 2010;112:1316-1324.

---

83. Morgan JP, Erny RE, Allen PD, et al. Abnormal intracellular calcium handling, a major cause of systolic and diastolic dysfunction in ventricular myocardium from patients with heart failure. *Circulation*. 1990;81(Suppl III):21-32.



- 
84. Carroll JD, Hess OM, Hirzel HO, et al. Left ventricular systolic and diastolic function in coronary artery disease: effects of revascularization on exercise-induced ischemia. *Circulation*. 1985;72:119-129.
- 
85. Weiss JL, Frederiksen JW, Weisfeldt ML. Hemodynamic determinants of the time course of fall in canine left ventricular pressure. *J Clin Invest*. 1976;58:751-760.
- 
86. Raff GL, Glantz SA. Volume loading slows left ventricular isovolumic relaxation rate: evidence of load-dependent relaxation in the intact dog heart. *Circ Res*. 1981;48:813-824.
- 
87. Serizawa T, Vogel WM, Apstein CS, et al. Comparison of acute alterations in left ventricular relaxation and diastolic chamber stiffness induced by hypoxia and ischemia. Role of myocardial oxygen supply-demand imbalance. *J Clin Invest*. 1981;68:91-102.
- 
88. Eichhorn P, Grimm J, Koch R, et al. Left ventricular relaxation in patients with left ventricular hypertrophy secondary to aortic valve disease. *Circulation*. 1982;65:1395-1404.
- 
89. Pagel PS, Kampine JP, Schmeling WT, et al. Alteration of left ventricular diastolic function by desflurane, isoflurane, and halothane in the chronically instrumented dog with autonomic nervous system blockade. *Anesthesiology*. 1991;74:1103-1114.
- 
90. Eichhorn EJ, Willard JE, Alvarez L, et al. Are contraction and relaxation coupled in patients with and without congestive heart failure? *Circulation*. 1992;85:2132-2139.
- 
91. Ohno M, Cheng C-P, Little WC. Mechanism of altered patterns of left ventricular filling during the development of congestive heart failure. *Circulation*. 1994;89:2241-2250.
- 
92. Glantz SA. Computing indices of diastolic stiffness has been counterproductive. *Fed Proc*. 1980;39:162-168.
- 
93. Mirsky I. Assessment of diastolic function: suggested methods and future considerations. *Circulation*. 1984;69:836-841.
- 
94. Myreng Y, Smiseth OA. Assessment of left ventricular relaxation by Doppler echocardiography. Comparison of isovolumic relaxation time and transmitral flow velocities with time constant of isovolumic relaxation. *Circulation*. 1990;81:260-266.
- 
95. Nishimura RA, Tajik AJ. Evaluation of diastolic filling of left ventricle in health and disease: Doppler echocardiography is the clinician's Rosetta stone. *J Am Coll Cardiol*. 1997;30:8-18.
- 
96. Nagueh SF, Appleton CP, Gillebert TC, et al. Recommendations for the evaluation of left ventricular diastolic function by echocardiography. *J Am Soc Echocardiogr*. 2009;22:107-133.
- 
97. Klein AL, Burstow DJ, Tajik AJ, et al. Effects of age on left ventricular dimensions and filling dynamics in 117 normal persons. *Mayo Clin Proc*. 1994;69: 212-224.
-

- 
98. Genovesi-Ebert A, Marabotti C, Palombo C, et al. Left ventricular filling: relationship with arterial blood pressure, left ventricular mass, age, heart rate, and body build. *J Hypertens*. 1991;9:345-353.
- 
99. Cohen GI, Petrolungo JF, Thomas JD, et al. A practical guide to assessment of ventricular diastolic function using Doppler echocardiography. *J Am Coll Cardiol*. 1996;27:1753-1760.
- 
100. Hurrell DG, Nishimura RA, Ilstrup DM, et al. Utility of preload alteration in assessment of left ventricular filling pressure by Doppler echocardiography: a simultaneous catheterization and Doppler echocardiographic study. *J Am Coll Cardiol*. 1997;30:459-467.
- 
101. Rakowski H, Appleton C, Chan KL, et al. Canadian consensus recommendations for the measurement and reporting of diastolic dysfunction by echocardiography: from the Investigators of Consensus on Diastolic Dysfunction by Echocardiography. *J Am Soc Echocardiogr*. 1996;9:736-760.
- 
102. Dini FL, Dell'Anna R, Micheli A, et al. Impact of blunted pulmonary venous flow on the outcome of patients with left ventricular systolic dysfunction secondary to either ischemic or idiopathic dilated cardiomyopathy. *Am J Cardiol*. 2000;85:1455-1460.
- 
103. Smiseth OA, Thompson CR, Lohavanichbutr K, et al. The pulmonary venous systolic flow pulse. Its origin and relationship to left atrial pressure. *J Am Coll Cardiol*. 1999;34:802-809.
- 
104. Fujii K, Ozaki M, Yamagishi T, et al. Effect of left ventricular contractile performance on passive left atrial filling: clinical study using radionuclide angiography. *Clin Cardiol*. 1994;17:258-262.
- 
105. Appleton CP, Gonzalez MS, Basnight MA. Relationship of left atrial pressure and pulmonary venous flow velocities: importance of baseline mitral and pulmonary venous flow velocity patterns in lightly sedated dogs. *J Am Soc Echocardiogr*. 1994;7:264-275.
- 
106. Keren G, Bier A, Sherez J, et al. Atrial contraction is an important determinant of pulmonary venous flow. *J Am Coll Cardiol*. 1986;7:693-695.
- 
107. Garcia MJ, Thomas JD, Klein AL. New Doppler echocardiographic applications for the study of diastolic function. *J Am Coll Cardiol*. 1998;32:865-875.
- 
108. Takatsuji H, Mikami T, Urasawa K, et al. A new approach for evaluation of left ventricular diastolic function: spatial and temporal analysis of left ventricular filling flow propagation by color M-mode Doppler echocardiography. *J Am Coll Cardiol*. 1996;27:365-371.
- 
109. Watkins MW, LeWinter MM. Physiologic role of the normal pericardium. *Annu Rev Med*. 1993;44:171-180.
- 
110. Maruyama Y, Ashikawa K, Isoyama S, et al. Mechanical interactions between four heart chambers with and without the pericardium in canine hearts. *Circ Res*. 1982;50:86-100.
-

111. Refsum H, Junemann M, Lipton MJ, Skioldebrand C, Carlsson E, Tyberg JV. Ventricular diastolic pressure-volume relations and the pericardium. Effects of changes in blood volume and pericardial effusion in dogs. *Circulation*. 1981;64:997-1004.
- 
112. Junemann M, Smiseth OA, Refsum H, et al. Quantification of effect of pericardium on LV diastolic PV relation in dogs. *Am J Physiol*. 1987;252:H963-H968.
- 
113. Santamore WP, Dell'Italia LJ. Ventricular interdependence: significant left ventricular contributions to right ventricular systolic function. *Prog Cardiovasc Dis*. 1998;40:289-308.
- 
114. Weber KT, Janicki JS, Shroff S, et al. Contractile mechanics and interaction of the right and left ventricles. *Am J Cardiol*. 1981;47:686-695.
- 
115. Gonzalez MS, Basnight MA, Appleton CP. Experimental cardiac tamponade: a hemodynamic and Doppler echocardiographic reexamination of the relation of right and left heart ejection dynamics to the phase of respiration. *J Am Coll Cardiol*. 1991;18:243-252.
- 
116. Pinsky MR. Functional hemodynamic monitoring. *Crit Care Clin*. 2015;31:89-111.
- 
117. Santamore WP, Heckman JL, Bove AA. Right and left ventricular pressure-volume response to elevated pericardial pressure. *Am Rev Respir Dis*. 1986;134:101-107.
- 
118. Santamore WP, Bartlett R, Van Buren SJ, et al. Ventricular coupling in constrictive pericarditis. *Circulation*. 1986;74:597-602.
- 
119. Goldman S, Olajos M, Morkin E. Comparison of left atrial and left ventricular performance in conscious dogs. *Cardiovasc Res*. 1984;18:604-612.
- 
120. Payne RM, Stone HL, Engelken EJ. Atrial function during volume loading. *J Appl Physiol*. 1971;31:326-331.
- 
121. Dernellis J, Tsiamis E, Stefanadis C, et al. Effects of postural changes on left atrial function in patients with hypertrophic cardiomyopathy. *Am Heart J*. 1998;136:982-987.
- 
122. Gare M, Schwabe DA, Hettrick DA, et al. Desflurane, sevoflurane, and isoflurane affect left atrial active and passive mechanical properties and impair left atrial-left ventricular coupling in vivo. Analysis using pressure-volume relations. *Anesthesiology*. 2001;95:689-698.
- 
123. Prioli A, Marino P, Lanzoni L, et al. Increasing degrees of left ventricular filling impairment modulate left atrial function in humans. *Am J Cardiol* 1998;82:756-761.
- 
124. Ito T, Suwa M, Kobashi A, et al. Reversible left atrial dysfunction possibly due to afterload mismatch in patients with left ventricular dysfunction. *J Am Soc Echocardiogr*. 1998;11:274-279.
- 
125. Plehn JF, Southworth J, Cornwell GG III. Brief report: atrial systolic failure in primary amyloidosis. *N*

126. Tabata T, Oki T, Yamada H, et al. Role of left atrial appendage in left atrial reservoir function as evaluated by left atrial appendage clamping during cardiac surgery. *Am J Cardiol.* 1998;81:327-332.

---

127. Hoit BD, Shao Y, Tsai LM, et al. Altered left atrial compliance after atrial appendectomy. Influence on left atrial and ventricular filling. *Circ Res.* 1993; 72:167-175.

---

128. Nishikawa Y, Roberts JP, Tan P, et al. Effect of dynamic exercise on left atrial function in conscious dogs. *J Physiol.* 1994;481:457-468.

---

129. Toutouzas K, Trikas A, Pitsavos C, et al. Echocardiographic features of left atrium in elite male athletes. *Am J Cardiol.* 1996;78:1314-1317.

---

130. Triposkiadis F, Tentolouris K, Androulakis A, et al. Left atrial mechanical function in the healthy elderly: new insights from a combined assessment of changes in atrial volume and transmitral flow velocity. *J Am Soc Echocardiogr.* 1995;8:801-809.

---

131. Nishigaki K, Arakawa M, Miwa H, et al. A study of left atrial transport function. Effect of age or left ventricular ejection fraction on left atrial storage function. *Angiology.* 1994;45:953-962.

---

132. Zuccala G, Cocchi A, Lattanzio F, et al. Effect of age on left atrial function in patients with coronary artery disease. *Cardiology.* 1994;85:8-13.

---